

intRinsic: an R package for model-based estimation of the intrinsic dimension of a dataset

Francesco Denti

fdenti@uci.edu

University of California, Irvine

February 4, 2022

The estimation of the intrinsic dimension of a dataset is a fundamental step in most dimensionality reduction techniques. This article illustrates `intRinsic`, an R package that implements novel state-of-the-art likelihood-based estimators of the intrinsic dimension of a dataset. In order to make these novel estimators easily accessible, the package contains a small number of high-level functions that rely on a broader set of efficient, low-level routines. Generally speaking, `intRinsic` encompasses models that fall into two categories: homogeneous and heterogeneous intrinsic dimension estimators. The first category contains the `TWO-NN` model, an estimator derived from the distributional properties of the ratios of the distances between each data point and its first two of nearest neighbors. The functions dedicated to this method carry out inference under both the frequentist and Bayesian frameworks. In the second category, we find `Hidalgo`, a Bayesian mixture model, for which an efficient Gibbs sampler is implemented. After presenting the theoretical background, we demonstrate the performance of the models on simulated datasets. This way, we can facilitate the exposition by immediately assessing the validity of the results. Then, we employ the package to study the intrinsic dimension of the `Alon` dataset, obtained from a famous microarray experiment. We show how the estimation of homogeneous and heterogeneous intrinsic dimensions allows us to gain valuable insights into the topological structure of a dataset.

Keywords: intrinsic dimension, nearest neighbors, likelihood-based method, heterogeneous intrinsic dimension, bayesian mixture model, R

1 Introduction

Statisticians and data scientists are often called to manipulate, analyze, and summarize datasets that present high-dimensional and elaborate dependency structures. In multiple cases, these large datasets contain variables characterized by a considerable amount of redundant information. One can exploit these redundancies to represent a large dataset on a much lower-dimensional scale. This summarization procedure, called *dimensionality reduction*, is a fundamental step in many statistical analyses. For example, dimensionality reduction techniques make otherwise challenging tasks as large data manipulation and visualization feasible by reducing computational time and memory requirements.

More formally, dimensionality reduction is possible whenever the data points take place on one or more manifolds characterized by a lower dimension than what has been originally observed.

We call the dimension of a latent, potentially non-linear manifold the *intrinsic dimension* (`id`). Several other definitions of `id` exist in the literature. For example, we can see the `id` as the minimal number of parameters needed to represent all the information contained in the data without significant information loss [Ansuini et al., 2019, Rozza et al., 2011, Bennett, 1969]. Intuitively, the `id` is an indicator of the complexity of the features of a dataset. It is a necessary piece of information to have before attempting to perform any dimensionality reduction, manifold learning, or visualization tasks. Indeed, most dimensionality reduction methods would be worthless without a reliable estimate of the true `id` they need to target: an underestimated `id` value can cause needless information loss. At the same time, the reverse can lead to an unnecessary waste of time and computational resources [Hino et al., 2017].

Over the past few decades, a vast number of methods for `id` estimation and dimensionality reduction have been developed. The algorithms can be broadly classified into two main categories: projection and geometric approaches. The former maps the original data to a lower-dimensional space. The projection function can be linear, as in the case of Principal Component Analysis (PCA) [Hotelling, 1933] or nonlinear, as in the case of Locally Linear Embedding [Roweis and Lawrence, 2000], Isomap [Tenenbaum et al., 2000], and the tSNE [Laurens and Geoffrey, 2009]. For more examples, see Jolliffe and Cadima [2016] and the references therein. In consequence, there is a plethora of R packages that implement these types of algorithms. To mention some examples, one can use the packages `RDRToolbox` [Bartenhagen, 2020], `lle` [Kayo, 2006], `Rtsne` [Krijthe, 2015], and the classic `princomp()` function from the default package `stats`.

Geometric approaches rely instead on the topology of a dataset, exploiting the properties of the distances between data points. Within this family, we can find fractal methods [Falconer, 2003], graphical methods [Costa and Hero, 2004], model-based likelihood approaches [Levina and Bickel, 2005], and methods based on nearest neighbors distances [Pettis et al., 1979]. Also in this case, numerous packages are available: for example, for fractal methods alone there are `fractaldim` [Sevcikova et al., 2014], `nonlinearTseries` [Garcia, 2020], and `tseriesChaos` [Di Narzo, 2019], among others. For a recent review of the methodologies used for `id` estimation we refer to Campadelli et al. [2015].

Given the abundance of approaches in this area, several R developers have also attempted to provide unifying collections of dimensionality reduction and `id` estimation techniques. For example, remarkable ensembles of methodologies are implemented in the packages `ider` [Hino, 2017], `dimred` and `coRanking` [Kraemer et al., 2018], `dyndimred` [Cannoodt and Saelens, 2020], `IDmining` [Golay and Kanevski, 2017], and `intrinsicDimension` [Johnsson and Lund University, 2019]. Among these proposals, the package `Rdimtools` [You, 2020b] stands out, implementing 150 different algorithms, 17 of which are exclusively dedicated to `id` estimation [You, 2020a].

In this paper, we introduce and discuss the R package `intRinsic` (version 0.2.0). The package is openly available from the Comprehensive R Archive Network (CRAN) at <https://CRAN.R-project.org/package=intRinsic>, and can be easily installed by running

```
R> install.packages("intRinsic")
```

Future developments and updates will be uploaded both on CRAN and on GitHub at <https://github.com/Fradenti/intRinsic>.

The package implements the `TWO-NN`, `Gride`, and `Hidalgo` models, three state-of-the-art `id` estimators recently introduced in Facco et al. [2017], Denti et al. [2021] and Allegra et al. [2020], respectively. These methods are likelihood-based estimators that rely on the theoretical properties of the distances among the nearest neighbors. The first two models yield an estimate of a global, unique `id` of a dataset and are implemented under both the frequentist and Bayesian paradigms. One can also exploit these models to study how the `id` of the dataset depends on the scale of the neighborhood considered for its estimation. `Hidalgo`, on the other hand,

is a Bayesian mixture model that allows for the estimation of clusters of points characterized by heterogeneous `ids`. In this article, we focus our attention on the exposition of `TWO-NN` and `Hidalgo`, and we discuss the pros and cons of both models with the aid of simulated data. More details about the additional routines implemented in our package, such as `Gride`, are reported in Section A of the Appendix. In Section B of the Appendix, we elaborate more on the strengths and weaknesses of the methods implemented in `intRinsic` in comparison to the other existing packages.

Broadly speaking, the package contains two sets of functions, organized into high-level and low-level routines. The former set contains user-friendly and straightforward R functions. Our goal is to make the package as accessible and intuitive as possible by automating most tasks. The low-level routines represent the core of the package, and they are not exported. The most computationally-intensive low-level functions are written in C++, exploiting the interface with R provided by the packages `Rcpp` and `RcppArmadillo` [Eddelbuettel and François, 2011, Eddelbuettel and Sanderson, 2014]. The C++ implementation considerably speeds up time-consuming tasks, like running the Gibbs sampler for the Bayesian mixture model `Hidalgo`. Moreover, `intRinsic` is well integrated with external R packages. For example, we enriched the package’s functionalities defining ad-hoc methods for generic functions like `autoplot()` from the `ggplot2` package [Wickham, 2016] to produce the appropriate graphical outputs.

The article is structured as follows. Section 2 introduces and describes the theoretical background of the `TWO-NN` and `Hidalgo` methods. Section 3 illustrates the basic usage of the implemented routines on simulated data. We show how to obtain, manipulate, and interpret the different outputs. Additionally, we assess the robustness of the methods by monitoring how the results vary when the input parameters change. Section 4 presents an applications to a famous real microarray datasets. Finally, Section 5 concludes discussing future directions and potential extensions to the package.

2 The modeling background

Let \mathbf{X} be a dataset with n data points measured over D variables. We denote each observation as $x_i \in \mathbb{R}^D$. Despite being observed over a D -dimensional space, we suppose that the points take place on a latent manifold \mathcal{M} with intrinsic dimension (`id` from now on) $d \leq D$. Generally, we expect that $d \ll D$. Thus, we postulate that a low-dimensional data-generating mechanism can accurately describe the dataset.

Then, consider a single data point x_i . Starting from this point, one can order the remaining $n - 1$ observations according to their distance from x_i . This way, we obtain a list of nearest neighbors (NNs) of increasing order. Formally, let $\Delta : \mathbb{R}^D \times \mathbb{R}^D \rightarrow \mathbb{R}^+$ be a generic distance function between data points. We denote with $x_i^{(l)}$ the l -th NN of x_i and with $r_{i,l} = \Delta(x_i, x_i^{(l)})$ their distance, for $l = 1, \dots, n - 1$. Given the sequence of NNs for each data point, we can define the *volume of the hyper-spherical shell enclosed between two successive neighbors of x_i* as

$$\nu_{i,l} = \omega_d \left(r_{i,l}^d - r_{i,l-1}^d \right), \quad \text{for } l = 1, \dots, n - 1, \text{ and } i = 1, \dots, n, \quad (1)$$

where d is the dimensionality of the latent manifold in which the points are embedded (the `id`) and ω_d is the volume of the d -dimensional hyper-sphere with unitary radius. For this formula to hold, we need to set $x_{i,0} \equiv x_i$ and $r_{i,0} = 0$. Considering the two-dimensional case for simplicity, we provide a visual representation of the quantities involved in Figure 1 for $l = 1, 2$.

From a modeling perspective, we assume the dataset \mathbf{X} is a realization of a Poisson point process characterized by density function $\rho(x)$. Facco et al. [2017] showed that the hyper-spherical shells defined in Equation (1) are the multivariate extension of the well-known *inter-arrival times* [Kingman, 1992]. Therefore, they proved that under the assumption of homogeneity

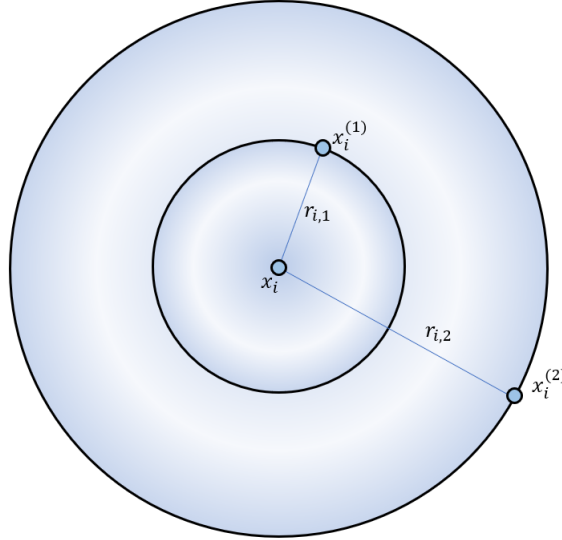


Figure 1: Pictorial representation in \mathbb{R}^2 of the first two NNs of point x_i and the corresponding distances. In two dimensions, the volume of the hyper-spherical shells $\nu_{i,1}$ and $\nu_{i,2}$ is equal to the surfaces of the first circle and the outer ring, respectively.

of the Poisson point process, i.e. $\rho(x) = \rho \ \forall x$, all the $\nu_{i,l}$'s are independently drawn from an Exponential distribution with rate equal to the density ρ : $\nu_{i,l} \sim \text{Exp}(\rho)$, for $l = 1, \dots, n-1$, and $i = 1, \dots, n$. This fundamental result motivates the derivation of the estimators we will introduce in the following sections.

2.1 The TWO-NN estimator

Building on the distribution of the hyper-spherical shells, [Facco et al. \[2017\]](#) noticed that, if the intensity of the Poisson point process is assumed to be constant on the scale of the second NN, the following distributional result holds:

$$\mu_{i,1,2} = \frac{r_{i,2}}{r_{i,1}} \sim \text{Pareto}(1, d), \quad \mu_i \in (1, +\infty) \quad i = 1, \dots, n. \quad (2)$$

In other words, if the intensity of the Poisson point process that generates the data can be regarded as locally constant (on the scale of the second NN), the ratio of the first two distances from the closest two NNs is Pareto distributed. Recall that the Pareto random variable is characterized by a scale parameter a , shape parameter b , and density function $f_X(x) = ab^a x^{-a-1}$ defined over $x \in [a, +\infty]$. Remarkably, Equation (2) states that the ratio $r_{i,2}/r_{i,1}$ follows a Pareto distribution with scale $a = 1$ and shape $b = d$, i.e., the shape parameter can be interpreted as the `id` of the data.

One can also attain more general results by considering ratios of distances with NNs of generic orders. A generalized ratios will be denoted with $\mu_{i,n_1,n_2} = \frac{r_{i,n_2}}{r_{i,n_1}}$ for $i = 1, \dots, n$, where n_1 and n_2 are the NN orders, integer numbers that need to comply with the following constraint: $1 \leq n_1 < n_2 \leq n$. In this paper, we will mainly focus on methods involving the ratio of the first two NN distances. The generalized ratios will be mentioned only when discussing the function `compute_mus()`. Therefore, for notational clarity, we will assume $\mu_i = \mu_{i,1,2}$ and $\boldsymbol{\mu} = (\mu_i)_{i=1}^n$. Once the vector $\boldsymbol{\mu}$ is computed, we can employ different estimators for the `id`. All of the following methods can be called via the `intrinsic` function `twonn()`. Examples about its usage can be found in Section 3.3.

Linear Estimator. [Facco et al. \[2017\]](#) proposed to estimate the `id` via the linearization of the Pareto c.d.f. $F(\mu_i) = (1 - \mu_i^{-d})$. The estimate \hat{d}_{OLS} is obtained as the solution of

$$-\log(1 - \hat{F}(\mu_{(i)})) = d \log(\mu_{(i)}), \quad (3)$$

where $\hat{F}(\cdot)$ denotes the empirical c.d.f. of the sample and the $\mu_{(i)}$'s are the ratios defined in Equation (2) sorted by increasing order. To obtain a more robust estimation, the authors suggested trimming from $\boldsymbol{\mu}$ a percentage c_{TR} of the most extreme values. This choice is justified because the extreme ratios often correspond to observations that do not comply with the local homogeneity assumption.

Maximum Likelihood Estimator. In a similar spirit, [Denti et al. \[2021\]](#) took advantage of the distributional results in Equation (2) to derive a simple Maximum Likelihood Estimator (MLE) and corresponding Confidence Interval (CI). Trivially, the (unbiased) MLE for the shape parameter of a Pareto distribution is given by:

$$\hat{d} = \frac{n-1}{\sum_i^n \log(\mu_i)}, \quad (4)$$

while the corresponding CI of level $(1-\alpha)$ is defined as

$$CI(d, 1-\alpha) = \left[\frac{\hat{d}}{q_{IG_{n,(n-1)}}^{1-\alpha/2}}, \frac{\hat{d}}{q_{IG_{n,(n-1)}}^{\alpha/2}} \right], \quad (5)$$

where $q_{IG_{a,b}}^{\alpha/2}$ denotes the quantile of order $\alpha/2$ of an Inverse-Gamma distribution of shape a and scale b .

Bayesian Estimator. It is also straightforward to derive an estimator according to a Bayesian perspective [[Denti et al., 2021](#)]. Indeed, one can specify a prior distribution on the shape parameter d . The most natural prior to choose is a conjugate $d \sim \text{Gamma}(a, b)$. It is immediate to derive the posterior distribution for the shape parameter:

$$d|\boldsymbol{\mu} \sim \text{Gamma}\left(a + n, b + \sum_{i=1}^n \log(\mu_i)\right). \quad (6)$$

With this method, one can obtain the principal quantiles of the posterior distribution, collecting point estimates and uncertainty quantification with a credible interval (CrI) of level α .

2.2 Hidalgo: the heterogeneous intrinsic dimension algorithm

The estimators we described in the previous sections implicitly assume that the `id` of a dataset is unique. However, considering a unique value for the `id` can often be limiting, especially when the data present complex dependence structures among variables. To extend the previous modeling framework, one can imagine that the data points are divided into clusters, each of them belonging to a latent manifold with its specific `id`. Allegra et al. (2020) employed this heterogeneous `id` estimation approach in their model: the heterogeneous `id` algorithm (**Hidalgo**). The authors proposed as density function of the generating point process a mixture of K distributions defined on K different latent manifolds, expressed as $\rho(\mathbf{x}) = \sum_{k=1}^K \pi_k \rho_k(\mathbf{x})$, where $\boldsymbol{\pi} = (\pi_1, \dots, \pi_K)$ is the vector of mixture weights. This assumption induces a mixture of Pareto distributions as the distribution of the ratios μ_i 's:

$$f(\mu_i|\mathbf{d}, \boldsymbol{\pi}) = \sum_{k=1}^K \pi_k d_k \mu_i^{-(d_k+1)}, \quad i = 1, \dots, n, \quad (7)$$

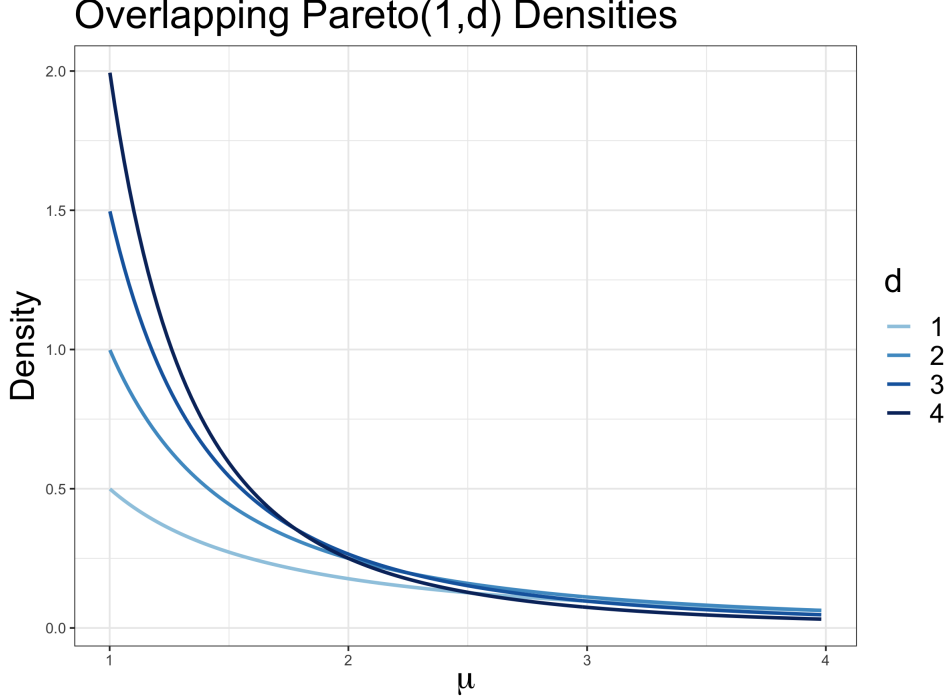


Figure 2: Density functions of $Pareto(1, d)$ distribution for different values of the shape parameter d .

where $\mathbf{d} = (d_1, \dots, d_K)$ is the vector of `id` parameters. Allegra et al. [2020] adopted a Bayesian perspective, specifying independent Gamma priors for each element of \mathbf{d} : $d_k \sim \text{Gamma}(a_d, b_d)$, and a Dirichlet prior for the mixture weights $\boldsymbol{\pi} \sim \text{Dirichlet}(\alpha_1, \dots, \alpha_K)$. Regarding the latter, we suggest to set $\alpha_1 = \dots = \alpha_K = \alpha < 0.05$, fitting a sparse mixture model as suggested by Malsiner-Walli et al. [2017]. This prior allows the data to populate only the necessary number of mixture components. Thus, the value K is seen as an upper bound on the number of active clusters $K^* < K$.

Unfortunately, a model-based clustering approach like the one presented in Equation (7) is ineffective at modeling the data. The problem lies in the fact that the different Pareto kernel densities constituting the mixture components are extremely similar and overlapping. Therefore, Pareto densities with varying shape parameters can fit the same data points equally well, compromising the clustering. Even when considering very diverse shape parameters, the right tails of the different Pareto distributions overlap to a great extent. This issue is evident in Figure 2, where we illustrate different examples of $Pareto(1, d)$ densities. Thus, the distributional similarity jeopardizes the cluster assignments of the data points and the consequent `ids` estimation.

To address this problem, Allegra et al. [2020] introduced a local homogeneity assumption, which postulates that points close to each other are more likely to be part of the same latent manifold. To incorporate this, the authors added an extra penalizing term in the likelihood. We now summarize their approach.

First, they introduced the latent membership labels $\mathbf{z} = (z_1, \dots, z_n)$ to assign each observation to a cluster, where $z_i = k$ means that the i -th observation was assigned to the k -th mixture component. Then, they defined the binary adjacency matrix $\mathcal{N}^{(q)}$, whose entries are $\mathcal{N}_{ij}^{(q)} = 1$ if the point x_j is among the q NNs of x_i and 0 otherwise. Finally, they assumed the following probabilities: $\mathbb{P}[\mathcal{N}_{ij}^{(q)} = 1 | z_i = z_j] = \zeta_1$, with $\zeta_1 > 0.5$ and $\mathbb{P}[\mathcal{N}_{ij}^{(q)} = 1 | z_i \neq z_j] = \zeta_0$, with

$\zeta_0 < 0.5$. These probabilities are incorporated in the following distributional constraints for the data point x_i : $\pi(\mathcal{N}_i^{(q)}|z) = \prod_{j=1}^n \zeta_0^{\mathbb{1}_{z_i \neq z_j}} \zeta_1^{\mathbb{1}_{z_i = z_j}} / \mathcal{Z}_i$, where \mathcal{Z}_i is the normalizing constant and $\mathbb{1}_A$ is the indicator function, equal to 1 when the event A is true, 0 otherwise. A more technical discussion of this model extension and the validity of the underlying hypothesis can be found in the Supplementary Material of [Allegra et al. \[2020\]](#). For simplicity, we assume $\zeta_0 = \zeta$ and $\zeta_1 = 1 - \zeta$. The model becomes

$$\mathcal{L}(\mu_i, \mathcal{N}^{(q)}|\mathbf{d}, \mathbf{z}, \zeta) = d_{z_i} \mu_i^{-(d_{z_i}+1)} \times \prod_{i=1}^n \frac{\zeta^{\mathbb{1}_{z_i \neq z_j}} (1 - \zeta)^{\mathbb{1}_{z_i = z_j}}}{\mathcal{Z}_i}, \quad z_i|\boldsymbol{\pi} \sim \text{Cat}_K(\boldsymbol{\pi}), \quad (8)$$

where Cat_K denotes a Categorical distribution over the set $\{1, \dots, K\}$. A closed-form for the posterior distribution is not available, so we rely on MCMC techniques to simulate a posterior sample.

The function `Hidalgo()` implements the Bayesian mixture model under the conjugate prior and two other alternative distributions. When the nominal dimension D is low, the unbounded support of a Gamma prior may provide unrealistic results, where the posterior distribution assigns positive density to the interval $(D, +\infty)$. [Santos-Fernandez et al. \[2021\]](#) proposed to employ a more informative prior for \mathbf{d} :

$$\pi(d_k) = \hat{\rho} \cdot d_k^{a-1} \exp^{-bd_k} \frac{\mathbb{1}_{(0,D)}}{\mathcal{C}_{a,b,D}} + (1 - \hat{\rho}) \cdot \delta_D(d_k) \quad \forall k, \quad (9)$$

where they denoted the normalizing constant of a $\text{Gamma}(a, b)$ truncated over $(0, D]$ with $\mathcal{C}_{a,b,D}$. That is, the prior distribution for d_k is a mixture between a truncated Gamma distribution over $(0, D]$ and a point mass located at D . The parameter ρ denotes the mixing proportion. When $\rho = 1$, the distribution in (9) reduces to a simple truncated Gamma. Both approaches are implemented in `intRinsic`, but we recommend using the latter. We report the details of the implemented Gibbs sampler in Section C of the Appendix.

3 Examples using intRinsic

This section illustrates and discusses the main routines of the `intRinsic` package. In the following, we will indicate the number of observations and the observed nominal dimension with `n` and `D`, respectively. Let us also represent with $\mathcal{N}_k(m, \Sigma)$ a multivariate Normal distribution of dimension k , mean m , and covariance matrix Σ . Moreover, let $\mathcal{U}_{(a,b)}^{(k)}$ represent a multivariate Uniform distribution with support (a, b) in k dimensions. Finally, we denote with \mathbb{I}_k an identity matrix of dimension k . We first load our package by running:

```
R> library(intRinsic)
```

3.1 Simulated Datasets

To illustrate how to apply the different `id` estimation techniques available in the package, we will make use of three simulated datasets: **Swissroll**, **HyperCube**, and **GaussMix**. This way, we can compare the results of the experiments with the ground truth. One can generate the exact replica of the three simulated datasets used in this paper by running the code reported below.

The first dataset, **Swissroll**, is obtained via the classical Swissroll transformation $\mathcal{S} : \mathbb{R}^2 \rightarrow \mathbb{R}^3$ defined as $\mathcal{S}(x, y) = (x \cos(x), y, x \sin(x))$. We sample all the pairs of points (x, y) from two independent Uniform distributions on $(0, 10)$. To simulate such a dataset, we can use the function `Swissroll()` in `intRinsic`, specifying the number of observations `n` as input parameter.

Name	n	D	id
Swissroll	1000	3	2
HyperCube	500	8	5
GaussMix	1500	5	?

Table 1: Summary of the dimensionality characteristics of the three simulated datasets.

```
R> set.seed(123456)
R> # Swissroll dataset
R> Swissroll <- Swissroll(n = 1000)
```

The second dataset, **HyperCube**, contains a cloud of points sampled from $\mathcal{U}_{(0,1)}^{(5)}$ embedded in an eight-dimensional space \mathbb{R}^8 .

```
R> # Five dimensional uniform distribution
R> HyperCube <- replicate(5, runif(500))
R> HyperCube <- cbind(HyperCube, 0, 0, 0)
R> colnames(HyperCube) <- paste0("V", 1:8)
R> HyperCube <- data.frame(HyperCube)
```

Lastly, the dataset **GaussMix** is the collection of data points generated from three different random variables, X_1, X_2 , and X_3 , embedded in a five-dimensional Euclidean space. The three random variables are distributed as

$$X_1 = 3X_0, \quad X_0 \sim \mathcal{N}_1(-5, 1); \quad X_2 \sim \mathcal{N}_3(0, \mathbb{I}_3); \quad X_3 \sim \mathcal{N}_5(5, \mathbb{I}_5).$$

```
R> # Mixture of three Gaussian
R> v1 <- rnorm(500, mean = -5, sd = 1)
R> v1 <- data.frame(V1 = v1, V2 = 3 * v1, V3 = 0, V4 = 0, V5 = 0)
R> v2 <- cbind(replicate(3, stats::rnorm(500)), 0, 0)
R> v3 <- replicate(5, stats::rnorm(500, 5))
R> v4 <- data.frame(rbind(v1, v2, v3))
R> GaussMix <- data.frame(v4)
R> class_GMix <- rep(c("A", "B", "C"), rep(500, 3))
```

Next, we need to establish what are the true values of the **id** for the different datasets. Scatterplots are useful exploratory tools to spot any clear dependence across the columns of a dataset. For example, if we plot all the possible two-dimensional scatterplots from the **Swissroll** dataset, we obtain Figure 3. From the different panels, it is evident that two of the three coordinates are free, and we can recover the last coordinate as a function of the others. Therefore, the **id** of **Swissroll** is equal to 2. Moreover, from the description of the data simulation, it is also evident that the **id** = 5 for the **HyperCube** dataset. However, it is not as simple to figure out the value of the true **id** for **GaussMix**, given the heterogeneity of its data generating mechanism. Table 1 summarizes the sample sizes along with the true nominal dimensions **D** and **ids** that characterize the three datasets.

3.2 Ratios of nearest neighbors distances

The ratios between distances of NNs constitute the core quantities on which the theoretical development presented in Section 2 is based. We can compute the ratios μ_i defined in Equations

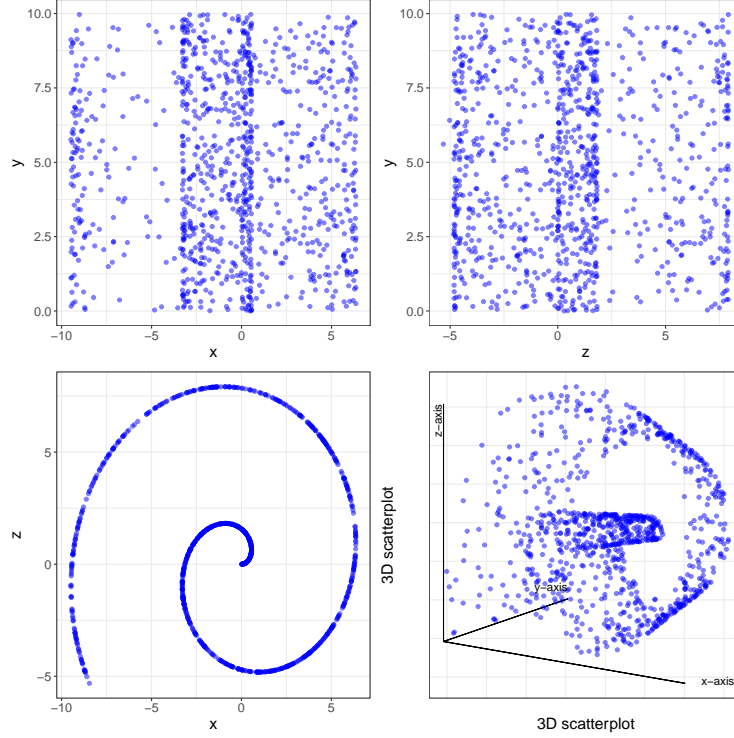


Figure 3: Scatterplots of the three variables in the `Swissroll` dataset. The dependence among the coordinates x and z is evident.

(2) with the function `compute_mus()`. However, note that the function can compute more general ratios μ_{n_1, n_2} , where $n_1 < n_2$, as presented in Section 2.1. In fact, the function needs the following arguments:

- **X**: a dataset of dimension $n \times D$ of which we want to compute the distance ratios;
- **dist_mat**: a $n \times n$ matrix containing the distances between data points;
- **n1**: the order of the closest nearest neighbor to consider. As default, $n_1 = 1$;
- **n2**: the order of the furthest nearest neighbor to consider; As default, $n_2 = 2$.

In addition to this list, there are two remaining arguments, **Nq** and **q**. They will be introduced later in Section 3.4, when we will discuss the application of `Hidalgo`. Note that the specification of **dist_mat** overrides the argument passed as **X**. Instead, if the distance matrix **dist_mat** is not specified, `generate_mus()` relies on the function `get.knn()` from the package `FNN` [Beygelzimer et al., 2019], which implements fast NN-search algorithms on the original dataset.

The main output of the function is the vector of ratios μ_{n_1, n_2} . To use the function, we can easily write:

```
R> mus_Swissroll <- compute_mus(X = Swissroll)
R> mus_HyperCube <- compute_mus(X = HyperCube)
R> mus_GaussMix <- compute_mus(X = GaussMix)
```

Calling the function with default arguments produces $\mu = \mu_{1,2}$. To explicitly compute generalized ratios, we need to specify the NN orders **n1** and **n2**. Here, we report two different examples:

n1	n2	Minimum	1st quartile	Median	Mean	3rd quartile	Maximum
1	2	1.0002	1.1032	1.3048	18.4239	1.9228	5874.3666
5	10	1.0234	1.1627	1.2858	1.5344	1.7043	6.9533
10	20	1.0472	1.1685	1.2613	1.4987	1.7250	4.0069

Table 2: Summary statistics for the **GaussMix** dataset. Each row corresponds to a different combination of NN orders.

```
R> mus_Swissroll_1 <- compute_mus(X = Swissroll, n1 = 5, n2 = 10)
R> mus_HyperCube_1 <- compute_mus(X = HyperCube, n1 = 5, n2 = 10)
R> mus_GaussMix_1 <- compute_mus(X = GaussMix, n1 = 5, n2 = 10)
```

and

```
R> mus_Swissroll_2 <- compute_mus(X = Swissroll, n1 = 10, n2 = 20)
R> mus_HyperCube_2 <- compute_mus(X = HyperCube, n1 = 10, n2 = 20)
R> mus_GaussMix_2 <- compute_mus(X = GaussMix, n1 = 10, n2 = 20)
```

The histograms of the computed ratios are reported in Figure 4. The panels in each row correspond to different datasets, while the effect of the varying NN orders is reported by column. The histograms are truncated over the interval $[0, 4]$ to ease the visualization. We see that the distributions present the right-skewed shape typical of the Pareto distribution. However, notice that some ratios could assume extreme values, especially when low values of NN orders are chosen. To provide an example, in Table 2 we display the summary statistics of the three vectors of ratios computed on **GaussMix**. The maximum in the first line has great magnitude, but it significantly reduces when higher NN orders are considered. It is also interesting to observe how the distribution for the ratios of **GaussMix** when $n1 = 10$ and $n2 = 20$ (bottom-right panel) is multimodal, a symptom of the presence of heterogeneous manifolds. We remark again that for the rest of the paper, we will focus on the **TWO-NN** and **Hidalgo** models. Therefore, we will only use `compute_mus()` in its default specification, simply computing $\boldsymbol{\mu} = (\mu_i)_{i=1}^n$. The ratios of NNs of generic order are necessary when using the **Grice** model. See Section A of the Appendix and Denti et al. [2021] for more details.

Finally, recall that the model is based on the assumption that a Poisson point process is the generating mechanism of the dataset. Ergo, the model cannot handle situations where ties among data points are present. From a more practical point of view, if $\exists i \neq j$ such that $x_i = x_j$, the computation of μ_i would be unfeasible, since $r_{i,1} = 0$. We devised the function `compute_mus()` to automatically detect if duplicates are present in a dataset. In that case, the function removes the duplicates and provides a warning. We showcase this behavior with a simple example with 3 unique data points:

```
R> Dummy_Data_with_replicates <- rbind(
+   c(1, 2, 3), c(1, 2, 3), # replicates
+   c(1, 4, 3), c(1, 4, 3), # replicates
+   c(1, 4, 5) )
R> mus_shorter <- compute_mus(X = Dummy_Data_with_replicates)
```

Warning:

Duplicates are present and will be removed.

Original sample size: 5. New sample size: 3.

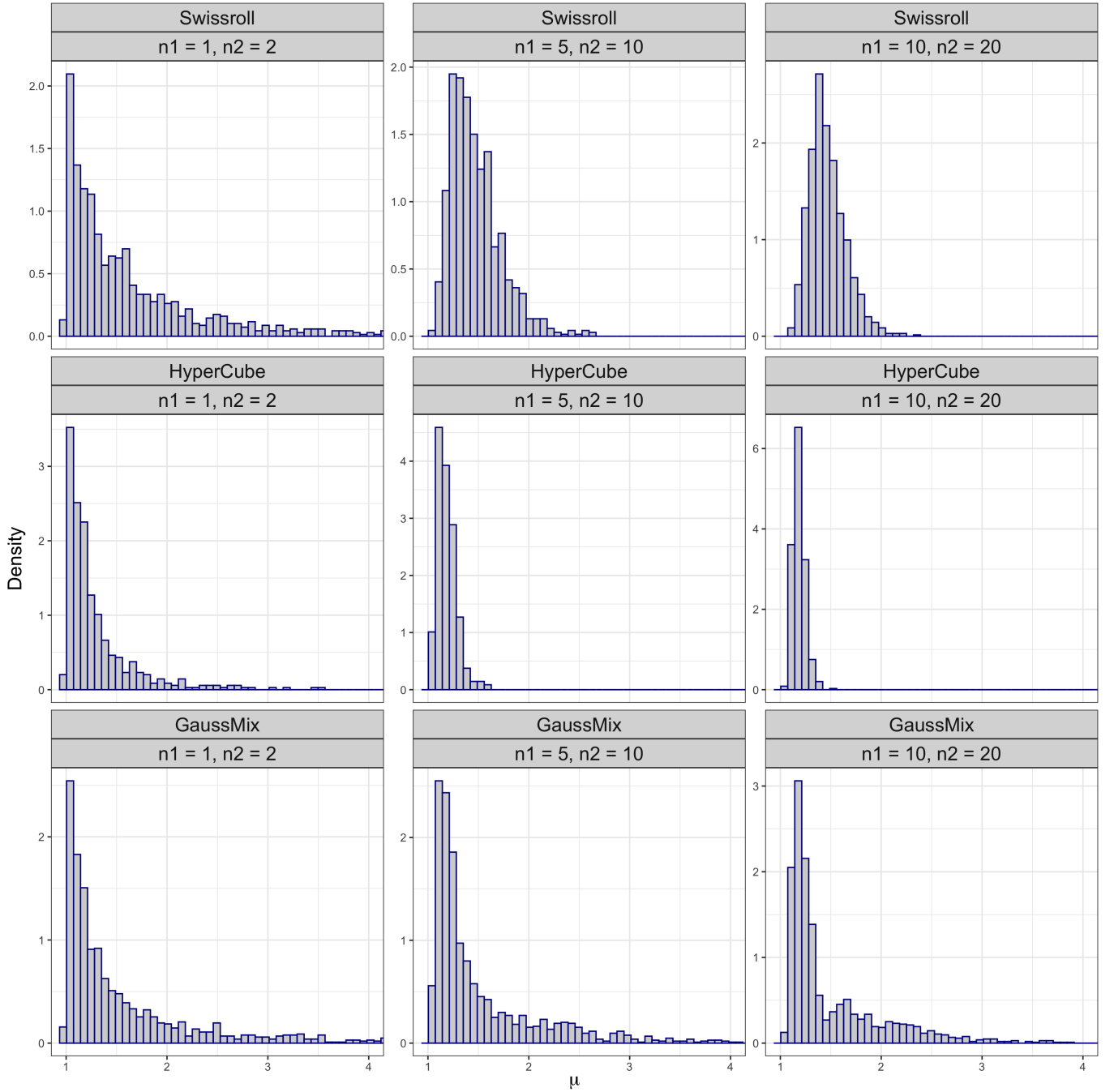


Figure 4: Histograms of the ratios $\mu_{n1,n2}$ for datasets **Swissroll**, **HyperCube**, and **GaussMix**. The shape of the histograms in the first column suggests that a Pareto distribution could be a good fit, according to the **TWO-NN** model.

The function `compute_mus()` is at the core of many other higher-level routines we use to estimate the `id`. In the following subsection, we show how to implement the **TWO-NN** model to obtain a point estimate of a global, homogeneous `id` accompanied by the corresponding confidence intervals (CI) or credible intervals (CrI).

3.3 Estimating a global intrinsic dimension with TWO-NN

In alignment with what presented in Section 2.1, we propose three methods to carry out inference on the `id`: the linear estimator, MLE, and Bayesian approach. The low-level functions that implement these methods are `twonn_mle()`, `twonn_linfit()`, and `twonn_bayes()`, respectively. These low-level functions can be called via the high-level function `twonn()`. Regardless of the preferred estimation method, the `twonn()` function takes the following arguments: the dataset `X` or the distance matrix `dist_mat` (refer to previous arguments specification for more details), along with

- `mus`: the vector of second-to-first NN distance ratios. If this argument is provided, `X` and `dist_mat` will be ignored;
- `method`: a string stating the preferred estimation method. Could be the maximum likelihood estimator (`"mle"`, the default), the estimation via least squares approach (`"linfit"`), or the estimation via Bayesian approach (`"bayes"`);
- `alpha`: the confidence level (for `"mle"` and `"linfit"`) or posterior probability included in the credible interval (`"bayes"`);
- `c_trimmed`: the proportions of most extreme ratios excluded from the analysis.

The object that the function returns is a list. The first element of the list always contains the estimates, while the others provide information about the chosen estimation process. The returned list is characterized by a class that varies according to the selected estimation method. Tailored R methods have been devised to extend the generic functions `print()` and `autoplot()`.

3.3.1 Linear Estimator

Here, we apply the linear estimator to the `Swissroll` dataset. As an example, we fit five linear models, by setting `method = "linfit"`, with different trimming proportions. Printing the output provides a quick summary of the estimation.

```
R> lin_1 <- twonn(X = Swissroll, method = "linfit", c_trimmed = 0)
R> lin_2 <- twonn(X = Swissroll, method = "linfit", c_trimmed = 0.001)
R> lin_3 <- twonn(X = Swissroll, method = "linfit", c_trimmed = 0.01)
R> lin_4 <- twonn(X = Swissroll, method = "linfit", c_trimmed = 0.05)
R> lin_5 <- twonn(X = Swissroll, method = "linfit", c_trimmed = 0.1)
R> # Example of output:
R> lin_2
```

Model: TWO-NN

Method: Least Square Estimation

Sample size: 1000, Obs. used: 999. Trimming proportion: 0.1%

ID estimates (confidence level: 0.95)

Lower Bound	Estimate	Upper Bound
-----:	-----:	-----:
1.986659	1.999682	2.012705

The results of these experiments are collected in Table 3. This first example allows us to comment on the trimming level to choose. Trimming the most extreme observations may be fundamental, since the estimate may be distorted by outliers. However, too much trimming would remove important information regarding the tail of the Pareto distribution, which is essential for

the estimation. As we can see, the estimates improve for very low levels of trimming, but start to degenerate as more than 10% of observations are removed from the dataset.

Trimming percentage	0%	0.1%	1%	5%	10%
Lower bound	1.9524	1.9867	2.2333	2.5709	2.9542
Estimate	1.9669	1.9997	2.2457	2.5988	2.9974
Upper bound	1.9814	2.0127	2.2581	2.6267	3.0407

Table 3: Point estimate and relative confidence intervals for the `id` values retrieved from the `Swissroll` dataset with the linear estimator. Each column displays the estimates for a specific trimming level.

We can also visually assess the goodness of fit via a dedicated `autoplot()` function, which plots the data and the relative regression line. The slope of the regression lines corresponds to the linear fit `id` estimates. For example, we obtain the plots in Figure 5 with the following two lines of code:

```
R> autoplot(lin_1, title = "No trimming")
R> autoplot(lin_5, title = "10% trimming")
```

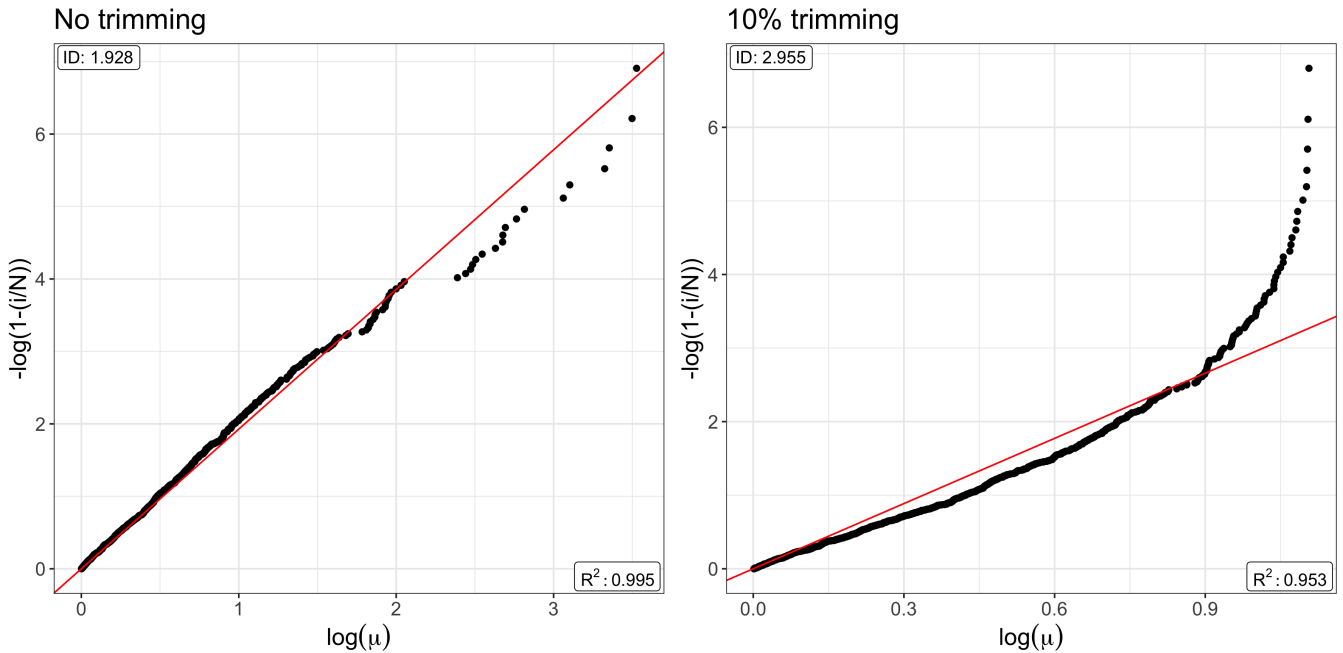


Figure 5: Linear regression fitted to the set of points $-\log(1 - \hat{F}(\mu_i)) = d \log(\mu_i)$ for the `Swissroll` dataset with no trimming (left panel) and 10% of trimmed observations (right panel).

3.3.2 Maximum Likelihood Estimator

A second way to obtain an `id` estimate, along with its confidence interval, is via MLE. The formulas implemented are presented in Equations (4) and (5). We compute the MLE by calling the low-level `twonn_mle()` function via `method = "mle"`. In addition to the previous arguments, one can also specify

- **unbiased:** logical, if TRUE the point estimate according to the unbiased estimator (where the numerator is $n - 1$, as in Equation (4)) is computed.

As an example, we will compute the `id` on `HyperCube` via MLE using different distance definitions: Euclidean, Manhattan, and Canberra. These distances are all implemented within `dist()` function in the `stats` package.

```
R> dist_Eucl_D2 <- as.matrix(stats::dist(HyperCube))
R> dist_Manh_D2 <- as.matrix(stats::dist(HyperCube, method = "manhattan"))
R> dist_Canb_D2 <- as.matrix(stats::dist(HyperCube, method = "canberra"))
```

Other distance matrices can be employed as well. In this example, we also show how the bounds of the CIs change by varying the confidence levels. We write:

```
R> mle_11 <- twonn(dist_mat = dist_Eucl_D2)
R> mle_12 <- twonn(dist_mat = dist_Eucl_D2, alpha = .99)
R> mle_21 <- twonn(dist_mat = dist_Manh_D2)
R> mle_22 <- twonn(dist_mat = dist_Manh_D2, alpha = .99)
R> mle_31 <- twonn(dist_mat = dist_Canb_D2)
R> mle_32 <- twonn(dist_mat = dist_Canb_D2, alpha = .99)
R> # Example of output:
R> mle_12
```

Model: TWO-NN

Method: MLE

Sample size: 500, Obs. used: 495. Trimming proportion: 1%

ID estimates (confidence level: 0.99)

```
| Lower Bound| Estimate| Upper Bound|
|-----:|-----:|-----:|
|    3.968082| 4.459427|    5.00273|
```

The results are summarized in Table 4. The type of distance can lead to differences in the results. Overall, the estimators agree with each other, obtaining values that are close to the ground truth.

dist()	Euclidean		Manhattan		Canberra	
α	0.95	0.99	0.95	0.99	0.95	0.99
Lower bound	4.0834	3.9681	4.0736	3.9585	4.6001	4.4701
Estimate	4.4594	4.4594	4.4487	4.4487	5.0237	5.0237
Upper bound	4.8706	5.0027	4.8588	4.9906	5.4868	5.6357

Table 4: MLE obtained from the TWO-NN model applied to the `HyperCube` dataset. Different distance functions and confidence level specifications are adopted.

3.3.3 Bayesian Estimation

The third option for `id` estimation is to adopt a Bayesian perspective and specify a prior distribution for the parameter d . To run the Bayesian estimates, we can call the low-level function

`twonn_bayes()` via `method = "bayes"` with `twonn()`. Along the aforementioned arguments, we can also specify:

- `a_d` and `b_d`: shape and rate parameters for the Gamma prior distribution on d . A vague specification is adopted as a default with `a_d = 0.001` and `b_d = 0.001`.

Differently from the previous two cases, recall that `alpha` in this context is assumed to be the probability contained in the credible interval computed on the posterior distribution. Along with the credible interval, the function outputs the posterior mean, median, and mode. In the following, four examples showcase the usage of this function on the `Swissroll` dataset with different combinations of credible interval levels and prior specifications. A summary of the results is reported in Table 5.

```
R> bay_1 <- twonn(X = Swissroll, method = "bayes")
R> bay_2 <- twonn(X = Swissroll, method = "bayes", alpha = 0.99)
R> bay_3 <- twonn(X = Swissroll, method = "bayes", a_d = 1, b_d = 1)
R> bay_4 <- twonn(X = Swissroll, method = "bayes", a_d = 1, b_d = 1, alpha = 0.99)
```

We can plot the posterior density of the parameter d using `autoplot()`, as displayed in Figure 6. When plotting an object of class `twonn_bayes`, we can also specify the following parameters:

- `plot_low` and `plot_upp`: lower and upper extremes of the support on which the posterior is evaluated;
- `by`: increment of the sequence going from `plot_low` to `plot_upp` that defines the support.

As an example, we compare the prior specification used for the object `bay_4` ($d \sim \text{Gamma}(1, 1)$) with a more informative one ($d \sim \text{Gamma}(10, 10)$) by writing:

```
R> bay_5 <- twonn(X = Swissroll, method = "bayes", a_d = 10, b_d = 10, alpha = 0.99)
R> # Example of output
R> bay_5
```

```
Model: TWO-NN
Method: Bayesian Estimation
Sample size: 1000, Obs. used: 990. Trimming proportion: 1%
Prior d ~ Gamma(10, 10)
Credibile Interval quantiles: 0.5%, 99.5%
Posterior ID estimates:
```

Lower Bound	Mean	Median	Mode	Upper Bound
-----:	-----:	-----:	-----:	-----:
1.991901	2.164113	2.163391	2.161949	2.344453

The posterior distribution is depicted in black, the prior in blue, and the dashed vertical red lines represent the estimates.

So far, we discussed methods to accurately and efficiently determine a global estimate of a dataset's `id`. Knowing the simulated data generating process, we could easily compare the obtained estimates with the ground truth for the `Swissroll` and `HyperCube` datasets. However, the same task is not immediate when dealing with `GaussMix`. For this dataset, it is unclear what value should represent the true `id` because the data points in `GaussMix` are generated from Gaussian distributions taking place on different manifolds of heterogeneous dimensions. This scenario is more likely to occur with datasets describing real phenomena, often characterized by complex dependencies, and it will be the focus of the next section.

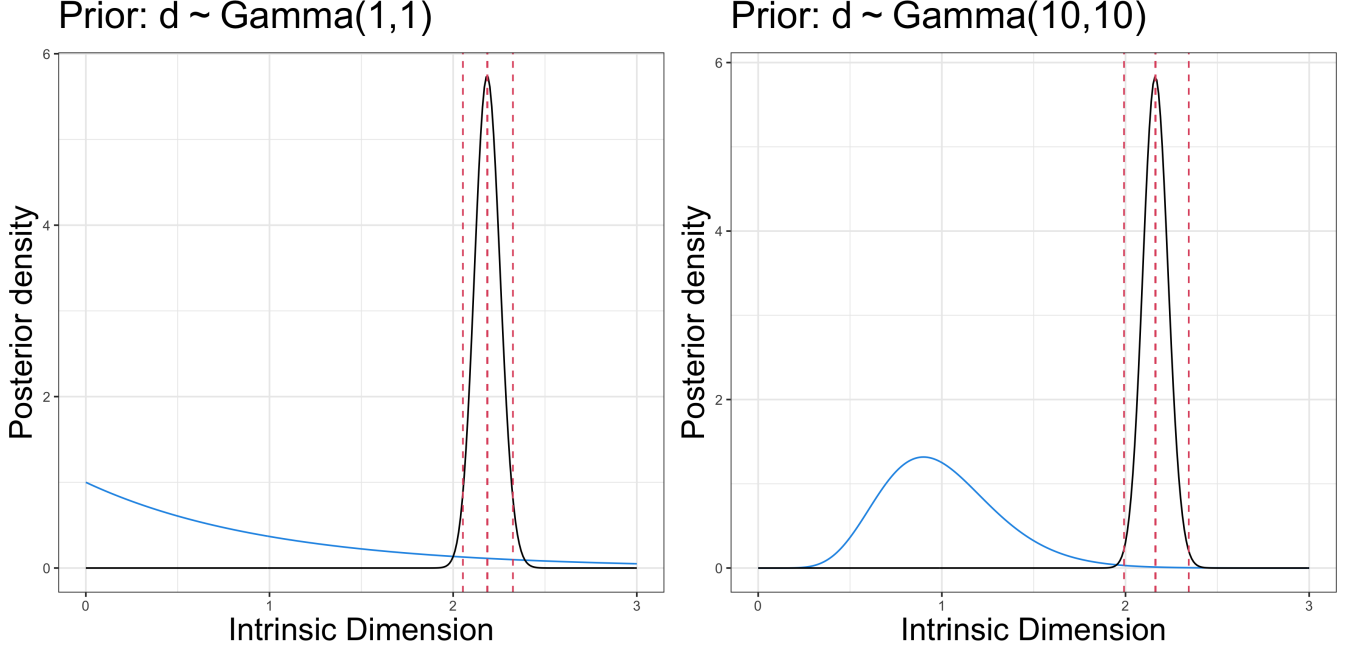


Figure 6: **Swissroll** dataset. Graphical representation of the posterior distribution (black line), prior distribution (blue line), and main quantiles and average (vertical dotted red lines) under $d \sim \text{Gamma}(1,1)$ (left panel) and $d \sim \text{Gamma}(10,10)$ (right panel) prior specifications.

Prior	Default		$d \sim \text{Gamma}(1,1)$	
α	0.95	0.99	0.95	0.99
Lower bound	2.0556	2.0147	2.0532	2.0124
Mean	2.1899	2.1899	2.1872	2.1872
Median	2.1891	2.1891	2.1865	2.1865
Mode	2.1876	2.1876	2.1850	2.1850
Upper bound	2.3284	2.3733	2.3255	2.3703

Table 5: Posterior estimates under the Bayesian specification according to different prior specifications and levels α of the credible interval.

3.4 Detecting manifolds with heterogeneous intrinsic dimensions using Hidalgo

3.4.1 Detecting the presence of multiple manifolds

In the context where the data may exhibit heterogeneous ids, we are facing two main challenges: (i) detect the actual presence of multiple manifolds in the data, and (ii) accurately estimate their ids. To tackle these problems, we start by applying the `twonn()` function to `GaussMix` with `method` equal to "linfit" and "mle".

```
R> mus_gm <- compute_mus(GaussMix)
R> twonn(mus = mus_gm, method = "linfit")
```

Model: TWO-NN

Method: Least Square Estimation

Sample size: 1500, Obs. used: 1485. Trimming proportion: 1%

```
ID estimates (confidence level: 0.95)
```

Lower Bound	Estimate	Upper Bound
-----:	-----:	-----:
1.438657	1.456325	1.473992

```
R> twonn(mus = mus_gm, method = "mle")
```

```
Model: TWO-NN
```

```
Method: MLE
```

```
Sample size: 1500, Obs. used: 1485. Trimming proportion: 1%
```

```
ID estimates (confidence level: 0.95)
```

Lower Bound	Estimate	Upper Bound
-----:	-----:	-----:
1.739329	1.830063	1.925601

The estimates obtained with the different methods do not agree. Figure 7 raises concerns about the appropriateness of a model postulating the existence of a single, global manifold. In the top panel of Figure 7, the data points are colored according to their generating mixture component. The sorted log-ratios present a non-linear pattern, where the slope values vary among the different mixture components A, B, and C.

Another empirical assessment can be given by the inspection of the evolution of the cumulative average distances between a point and its nearest neighbors. In other words, for each point x_i we consider the evolution of the ergodic mean of the sorted sequence of distances $(r_{i,0}, \dots, r_{i,n})$, given by $r_i(j) = \sum_{j=1}^J r_{i,j}/j \ \forall i, j$. Figure 8 displays the contrast between the HyperCube (left panel – exemplifying the homogeneous case) and GaussMix (right panel – representing the heterogeneous case) datasets. On the one hand, the left plot displays the ideal condition: there are no visible departures from the overall mean distance, which reassures us about the homogeneity assumption we made about the data. But, on the other hand, the right panel tells a different story. We immediately detect the different clusters in the data by focusing on their different starting values. The ergodic means remain approximately constant until the 500-th NNs, which corresponds to the size of each subgroup. The behavior of the cumulative means abruptly changes after the 500-th NN, negating the presence of a unique manifold. This type of plot provides an empirical but valuable overview of the structure between data points, highlighting the presence of clusters that may be reflecting the presence of multiple manifolds.

These visual assessments help detect signs of inappropriateness of the global id assumption. The most immediate approach to adopt in this case would be to divide the dataset into homogeneous subgroups and apply the TWO-NN estimator within each cluster. Such an approach is highlighted in the bottom panels of Figure 7. However, knowing ex-ante such well-separated groups is not a realistic expectation to have about actual data, and therefore we will rely on `Hidalgo()`, the Bayesian finite mixture model for heterogeneous id estimation described in Section 2.2.

3.4.2 Fitting the Hidalgo model

`Hidalgo` addresses the presence of multiple manifolds in the same dataset, yielding a vector of different estimated id values \mathbf{d} . As already discussed, estimating a mixture model with Pareto components is challenging because of their extensive overlap. A naive model-based estimation can lead to inaccurate results since there is no clear separation between the kernel densities.

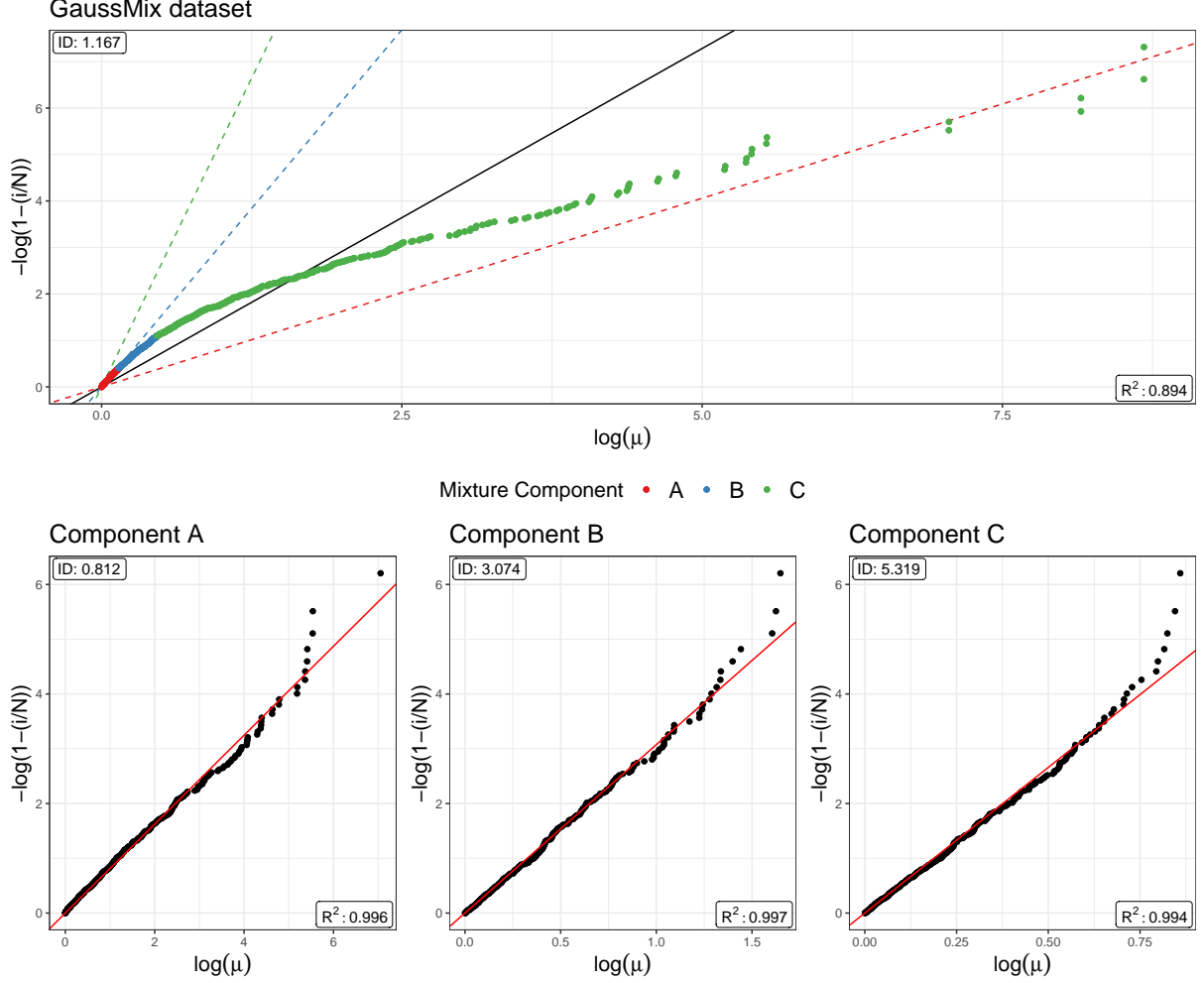


Figure 7: Linear estimators applied to the **GaussMix** dataset. In the top panel, the linear estimator is applied to the entire dataset. The points are colored according to the mixture component from which they originate, and the corresponding colored dashed lines represent the linear estimators applied to the subsets of points relative to each mixture component. The bottom three panels report the estimates within each single mixture component.

Therefore, we modify the classical Bayesian mixture using the likelihood stated in Equation (8). By introducing the extra term $\prod_{i=1}^n \pi(\mathcal{N}_i^{(q)} | \mathbf{z})$ into the likelihood, we can induce local homogeneity, which helps identify the model parameters.

The adjacency matrix $\mathcal{N}^{(q)}$ can be easily computed by specifying two additional arguments in the function `compute_mus()`:

- `Nq`: logical, if `TRUE`, the function adds the adjacency matrix to the output;
- `q`: integer, the number of NNs to be considered in the construction of the matrix $\mathcal{N}^{(q)}$. The default value is 3.

To provide an idea of the structure of the adjacency matrix $\mathcal{N}^{(q)}$, we report three examples obtained from a random sub-sample of the **GaussMix** dataset for increasing values of `q`. We display the heatmaps of the resulting matrices in Figure 9.

```
R> set.seed(12345)
```

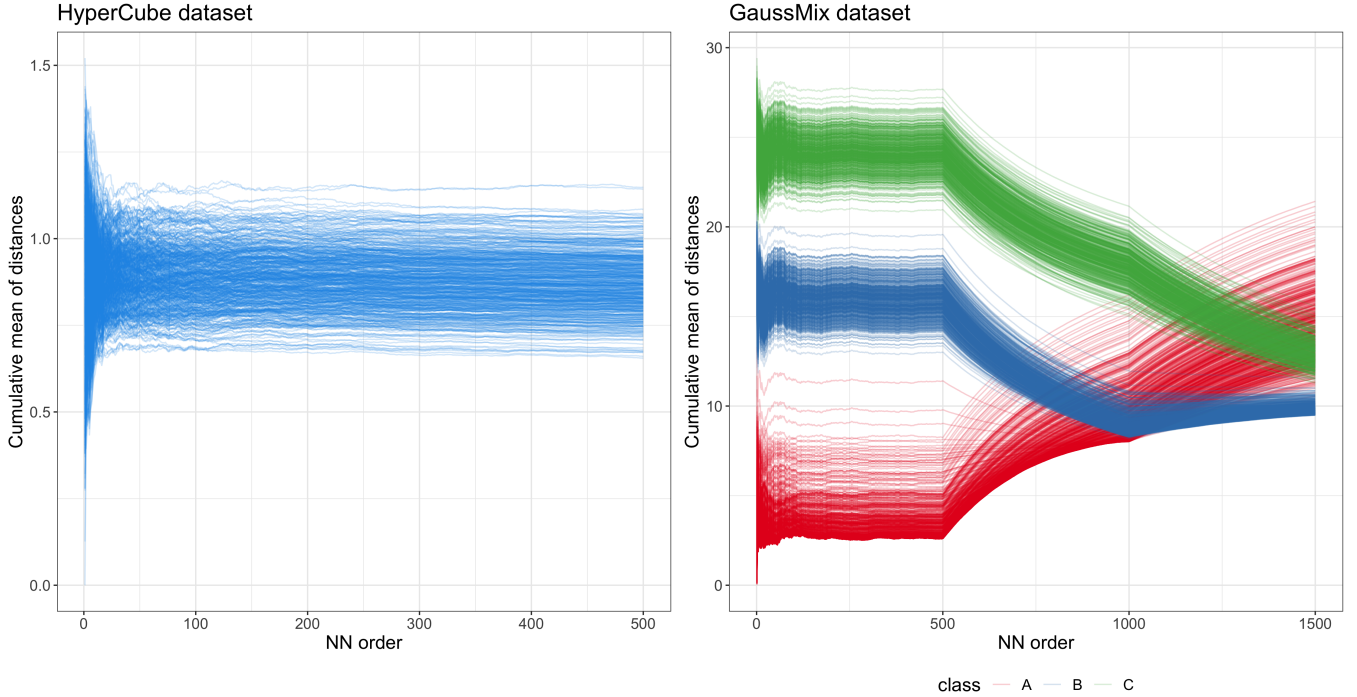



Figure 8: Evolution of the cumulative means of NN distances computed for all the observations in the **HyperCube** (left panel) and **GaussMix** (right panel) datasets. In the right panel, the colors highlight the different mixture components.

```
R> ind <- sort(sample(1:1500, 100, F))
R> Nq1 <- compute_mus(GaussMix[ind, ], Nq = T, q = 1)$NQ
R> Nq2 <- compute_mus(GaussMix[ind, ], Nq = T, q = 5)$NQ
R> Nq3 <- compute_mus(GaussMix[ind, ], Nq = T, q = 10)$NQ
```

As q increases, the binary matrix becomes more populated, uncovering the neighboring structure of the data points. [Allegra et al. \[2020\]](#) investigated how the performance of the model changes as q varies. They suggest fixing $q = 3$, a value that provides a good trade-off between the flexibility of the mixture allocations and local homogeneity.

Given this premise, we are now ready to discuss `Hidalgo()`, the high-level function that fits the Bayesian mixture. It implements the Gibbs sampler described in Section C of the Appendix, relying on low-level `Rcpp` routines. Also, the function internally calls `compute_mus()` to automatically generate the ratios of distances and the adjacency matrix needed to evaluate the likelihood from the data points.

The function has the following arguments: X , `dist_mat`, q , D , and

- K : integer, number of mixture components;
- `nsim`, `burn_in`, and `thinning`: number of MCMC iterations to collect, initial iterations to discard, and thinning interval, respectively;
- `verbose`: logical, if `TRUE`, the progress of the sampler is printed;
- ξ : real between 0 and 1, local homogeneity parameter. Default is 0.75;
- `alpha.Dirichlet`: hyperparameter of the Dirichlet prior on the mixture weights;
- `a0.d` and `b0.d`: shape and rate parameters of the Gamma prior on d . Here, the default is 1 for both values;

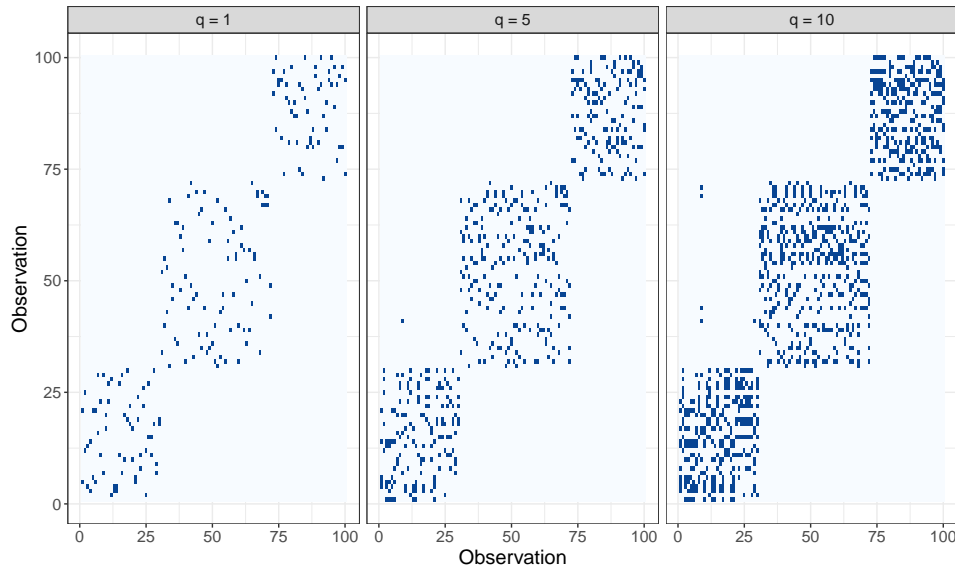


Figure 9: Heatmaps of the adjacency matrices $\mathcal{N}^{(q)}$ computed on a subset of observations of the **GaussMix** dataset. Different values of q are assumed.

- **prior_type**: string, type of Gamma prior on d which can be
 - **Conjugate**: a classic Gamma prior is adopted (default);
 - **Truncated**: a truncated Gamma prior on the interval $(0, D)$ is used. This specification is advised when dealing with datasets characterized by a small number of columns D , to avoid the estimated id exceeding the nominal dimension D ;
 - **Truncated_PointMass**: same as **Truncated**, but a point mass is placed on D . That is, the estimated id is allowed to be exactly equal to the nominal dimension D ;
- **pi_mass**: probability placed a priori on D when a **Truncated_PointMass** prior specification is chosen.

We apply the **Hidalgo** model on the **GaussMix** dataset with two different prior configurations: conjugate and truncated with point mass at $D = 5$. The code we used to run the models is:

```
R> set.seed(1234)
R> hid_fit <- Hidalgo(X = GaussMix, K = 10, alpha_Dirichlet = .05,
+                      nsim = 2000, burn_in = 2000, thinning = 5,
+                      verbose = FALSE)
R> set.seed(1234)
R> hid_fit_TR <- Hidalgo(X = GaussMix, K = 10, alpha_Dirichlet = .05,
+                          prior_type = "Truncated_PointMass", D = 5,
+                          nsim = 2000, burn_in = 2000, thinning = 5,
+                          verbose = FALSE)

R> # Output Example
R> hid_fit_TR
```

```
Model: Hidalgo
Method: Bayesian Estimation
Prior d ~ Gamma(1, 1), type = Truncated_PointMass
```

Prior on mixture weights: Dirichlet(0.05) with 10 mixture components
MCMC details:
Total iterations: 4000, Burn in: 2000, Elapsed time: 1.2289 mins

By using `alpha_Dirichlet = 0.05`, we have adopted a sparse mixture modeling approach in the spirit of Malsiner-Walli et al. [2016, 2017]. In principle, the sparse mixture approach would automatically let the data estimate the number of mixture components required. As a consequence, the argument `K` should be interpreted as an upper bound on the number of active clusters. Nonetheless, we stress that estimating well-separated clusters with Pareto kernels is challenging, and we will discuss how to analyze the output to perform proper inference. The output object `hid_fit` is a list of class `Hidalgo`, containing six elements:

- `cluster_prob`: matrix of dimension `nsim`×`K`. Each column contains the MCMC sample of the mixing weight for every mixture component;
- `membership_labels`: matrix of dimension `nsim`×`n`. Each column contains the MCMC sample of the membership labels for every observation;
- `id_raw`: matrix of dimension `nsim`×`K`. Each column contains the MCMC sample for the `id` estimated in every cluster;
- `id_postpr`: matrix of dimension `nsim`×`n`. It contains a chain for each observation, corrected for labels switching;
- `id_summary`: a matrix containing the values of posterior mean and the 5%, 25%, 50%, 75%, 95% quantiles for each observation;
- `recap`: a list with specifications passed to the function as inputs.

To inspect the output, we can employ the dedicated `autoplot()` function, devised for objects of class `Hidalgo`. There are several arguments that can be specified, producing different graphs. The most important is

- `type`: string that indicates the type of plot that is requested. It can be:
 - `raw_chains`: plot the MCMC and the ergodic means **not** corrected for label switching (default);
 - `point_estimates`: plot the posterior mean and median `id` for each observation, along with their credible intervals;
 - `class_plot`: plot the estimated `id` distributions stratified by the groups specified in an additional `class` vector;
 - `clustering`: plot the posterior co-clustering matrix. Rows and columns can be stratified by and external `class` and/or a clustering structure.

For example we can plot the raw chains of the two models with the aid of the `patchwork` package [Pedersen, 2020].

```
R> autoplot(hid_fit) / autoplot(hid_fit_TR)
```

The previous line produces Figure 10. Plotting the trace plots of the elements in `d` allows us to assess the convergence of the algorithm. We need to be aware that these chains may suffer from label-switching issues, preventing us from directly drawing inference from the MCMC output. Due to label-switching, mixture components can be discarded and emptied or repopulated across iterations. Indeed, Figure 10 shows the MCMC trace plots of the two models, with the ergodic means for each mixture component superimposed. Additionally, we can see that if no constraint is imposed on the support of the prior distribution for `d` (top panel), the posterior estimates can

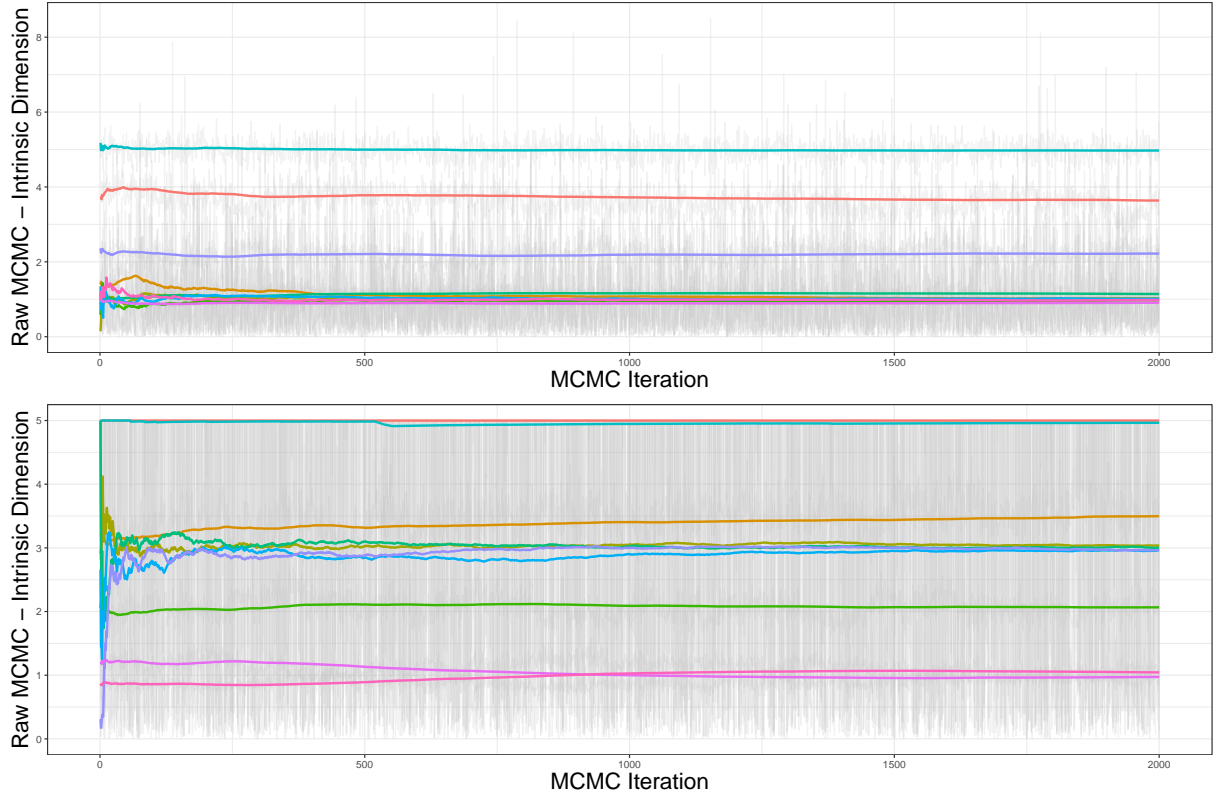


Figure 10: MCMC trace plots and superimposed ergodic means of components of the vector \mathbf{d} . Top panel: conjugate prior specification. Bottom panel: truncated with point mass prior specification.

exceed the nominal dimension $D = 5$ of the `GaussMix` dataset. However, this problem disappears when imposing a truncation on the prior support (bottom panel).

To address the label-switching issue and perform meaningful inference, the raw MCMC needs to be postprocessed. In Section D of the Appendix, we discuss the algorithm that is used to map the K chains to n observation-specific chains that can be employed for inference. The algorithm is already implemented in `Hidalgo()`, and produces the elements `id_postpr` and `id_summary` in the returned list. A visual summary of the post-processed estimates can be obtained via

```
R> autoplot(hid_fit, type = "point_estimates") +
+ autoplot(hid_fit_TR, type = "point_estimates")
```

The resulting plots are shown in Figure 11. The panels display the mean and median `id` estimates for each data point. Here, the separation of the data into different generating manifolds is evident. Also, we notice that some of the estimates in the conjugate case are incorrectly above the nominal value $D = 5$, once again justifying the need for a truncated prior.

3.4.3 Estimated clustering solutions

When dealing with a mixture model, it is natural to seek model-based clustering solutions. To this extent, the key source of information is the posterior similarity – or co-clustering – matrix (PSM). The entries of this matrix are computed as the proportion of times in which two observations have been assigned to the same mixture component across all the MCMC iterations. Thus, the PSM describes the underlying clustering structure of the data detected by `Hidalgo`. Given the

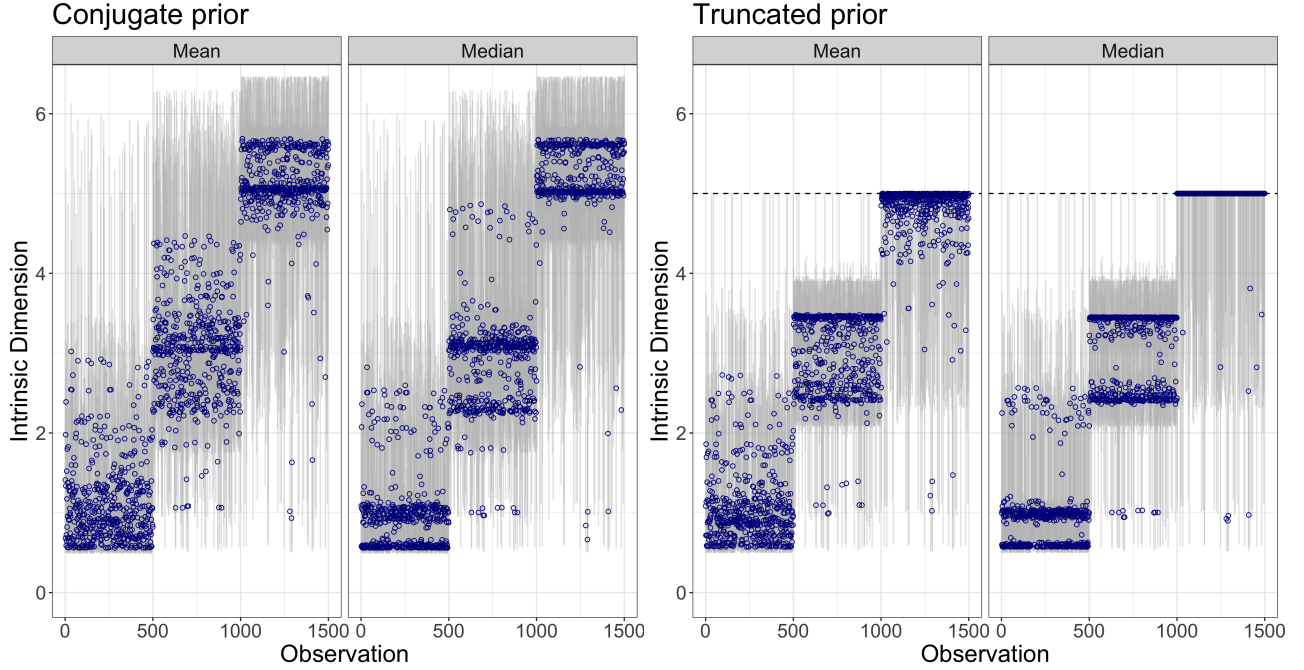


Figure 11: Observation-specific means (left panels) and median (right panels) `id` represented with blue dots. The gray bars represent a 90% credible interval. The two plots correspond to the two different prior specifications. The default plots were modified with `coord_cartesian(ylim = c(0, 6.3))` to highlight the effect of the truncation.

PSM, one can evaluate various loss functions on the space of the partitions. By minimizing the loss functions, we can retrieve the optimal partition of the dataset into clusters. To obtain such estimate, one can rely on the function `salso()` from the R packages `salso` [Dahl et al., 2021]. Otherwise, a faster alternative method proceeds by building a dendrogram from the dissimilarity matrix $1 - \text{PSM}$ and thresholds it to segment the data into a prespecified number of clusters K .

These approaches are implemented in the dedicated function `psm_and_cluster()` which takes as arguments, along the `object` output from the `Hidalgo()` function,

- **clustering_method**: string indicating the method to use to perform clustering. It can be "dendrogram" or "salso". The former method thresholds the dendrogram constructed from the dissimilarity matrix $1 - \text{PSM}$ to retrieve K clusters. The latter method estimates the optimal clustering by minimizing a loss function on the space of the partitions. The default loss function is the Variation of Information (VI);
- **K**: integer. If "dendrogram" is chosen, it is the number of clusters to recover with the thresholding of the dendrogram obtained from the PSM;
- **nCores**: integer, argument for the functions taken from `salso`. It represents the number of cores used to compute the PSM and the optimal clustering solution.

Additional arguments can be passed to personalize the partition estimation via `salso()`. Given the large sample size of the `GaussMix` dataset, we opt for the dendrogram approach, truncating the dendrogram at $K = 3$ groups. We highlight that relying on the minimization of a loss function is a more principled approach. However, the method can be misled by the strongly overlapping clusters estimated across the MCMC iterations, providing overly conservative solutions.

```
R> psm_cl <- psm_and_cluster(object = hid_fit_TR,
```

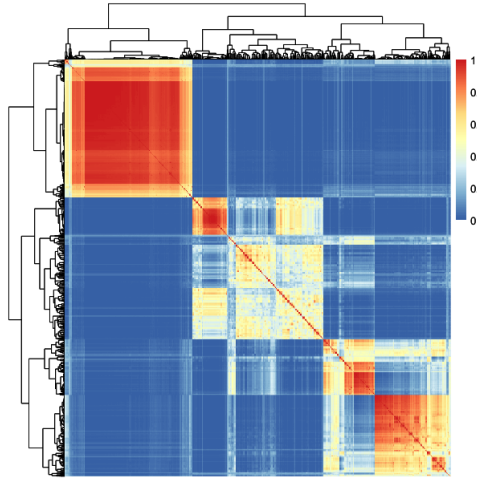


Figure 12: GaussMix dataset. Posterior co-clustering matrix computed from the output of the Hidalgo model.

```
+ clustering_method = "dendrogram",
+ K=3, nCores = 5)
R> # Example of output
R> psm_cl
```

Estimated clustering solution summary:

Method: dendrogram.
Retrieved clusters: 3.
Clustering frequencies:

Cluster 1	Cluster 2	Cluster 3
648	356	496

To visualize the results, we can also plot the PSM via `autoplot()` which, if `type = "clustering"`, directly calls `psm_and_cluster`.

```
R> autoplot(hid_fit_TR, type = "clustering")
```

As we can see from Figure 12, the model correctly detects the three clusters in the data. One can specify additional arguments in the `autoplot()` to stratify columns and rows according to external factors or the estimated clustering solution.

3.4.4 The presence of patterns in the data uncovered by the id

Once the observation-specific id chains are computed, we can investigate the presence of potential patterns between the estimates and given external variables. To explore these possible relations, we can use the function `id_by_class()`. Along with an object of class `Hidalgo`, we need to specify:

- **class:** factor, a variable used to stratify the id posterior estimates.

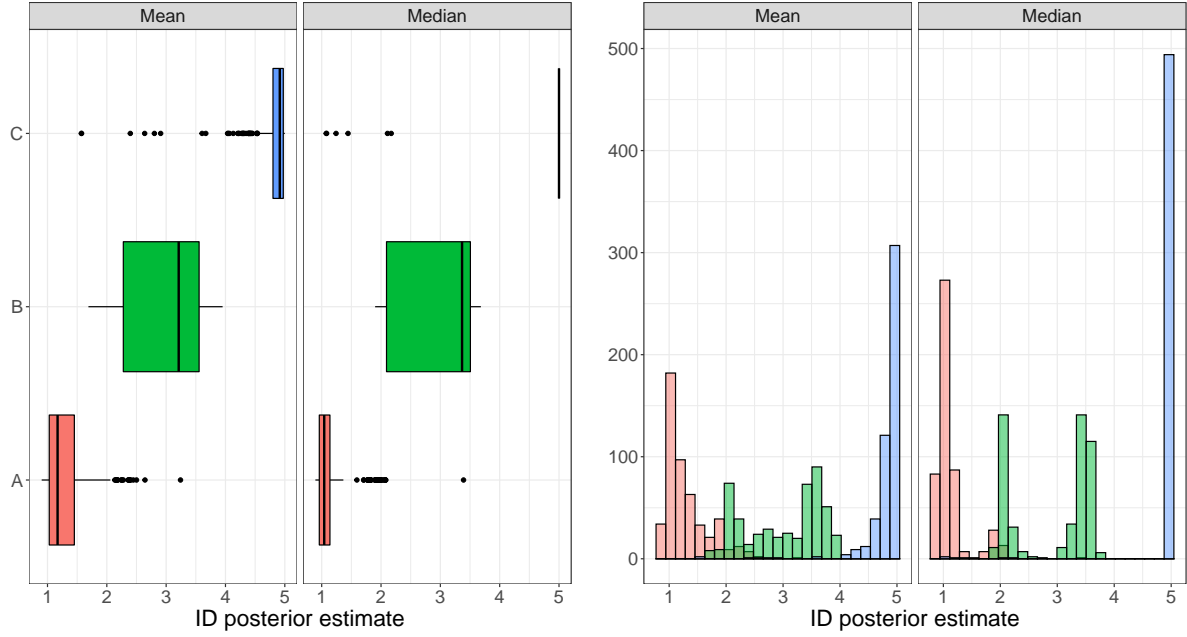


Figure 13: Two different types of graphs that the `autoplot()` method can produce (left panel: boxplots, right panel: histograms). The `ids` estimates of the `GaussMix` dataset are stratified according the generating distribution, as specified in the `class` argument.

```
R> id_by_class(object = hid_fit_TR, class = class_GMix)
```

	class	mean	median	sd
A	A	1.069257	0.9282385	0.4680442
B	B	2.963738	3.0577284	0.4947821
C	C	4.777659	4.9293029	0.4452653

The estimates in the three classes are very close to the ground truth. The same argument, `class`, can be passed to the `autoplot()` function, in combination with

- `class_plot_type`: string, if `type = "class_plot"`, one can visualize the stratified `id` estimates with a `"density"` plot or a `"histogram"`, or using `"boxplots"` or `"violin"` plots;
- `class`: a vector containing a class used to stratify the observations;

to visualize `id` estimates of the `GaussMix` dataset stratified by the generating manifold of the observations. This information is contained in `class_GMix`, which we pass as `class`. As an example of possible graphs, Figure 13 shows the stratified boxplots (left panel) and histograms (right panel).

```
R> autoplot(hid_fit_TR, type = "class", class = class_GMix,
+           class_plot_type = "boxplot") +
+ autoplot(hid_fit_TR, type = "class", class = class_GMix,
+           class_plot_type = "histogram")
```

We have introduced and discussed the principal functions of the `intrinsic` package concerning the `TWO-NN` and `Hidalgo` models. Employing simulated data with known `id`, we presented a pipeline to guide our analysis. In the next section, we present a real-data analysis, highlighting how the `id` estimation can be used to effectively reduce the size of a dataset while capturing and preserving important features.

4 Alon dataset: gene microarray measurements

In this section, we present a real-data example investigating the id of the Alon dataset. A copy of this famous microarray measurements table can be found in the R package `HiDimDA`. The dataset, first presented in Alon et al. [1999], contains microarray data for 2,000 genes measured on 62 patients. Among the patients, 40 were diagnosed with colon cancer and 22 were healthy subjects. A factor variable named `status` describes the patient health condition (coded as "Cancer" vs. "Healthy"). We store the gene measurements in the object `Xalon`, a matrix of nominal dimension $D = 2000$, with $n = 62$ observations. To load and prepare the data, we write:

```
R> data("AlonDS", package = "HiDimDA")
R> status <- factor(AlonDS$grouping, labels = c("Cancer", "Healthy"))
R> Xalon <- as.matrix(AlonDS[, -1])
```

To obtain a visual summary of the dataset, we plot the heatmap of the log-data values annotated by `status`. The result is shown in Figure 14. No clear structure is immediately visible.

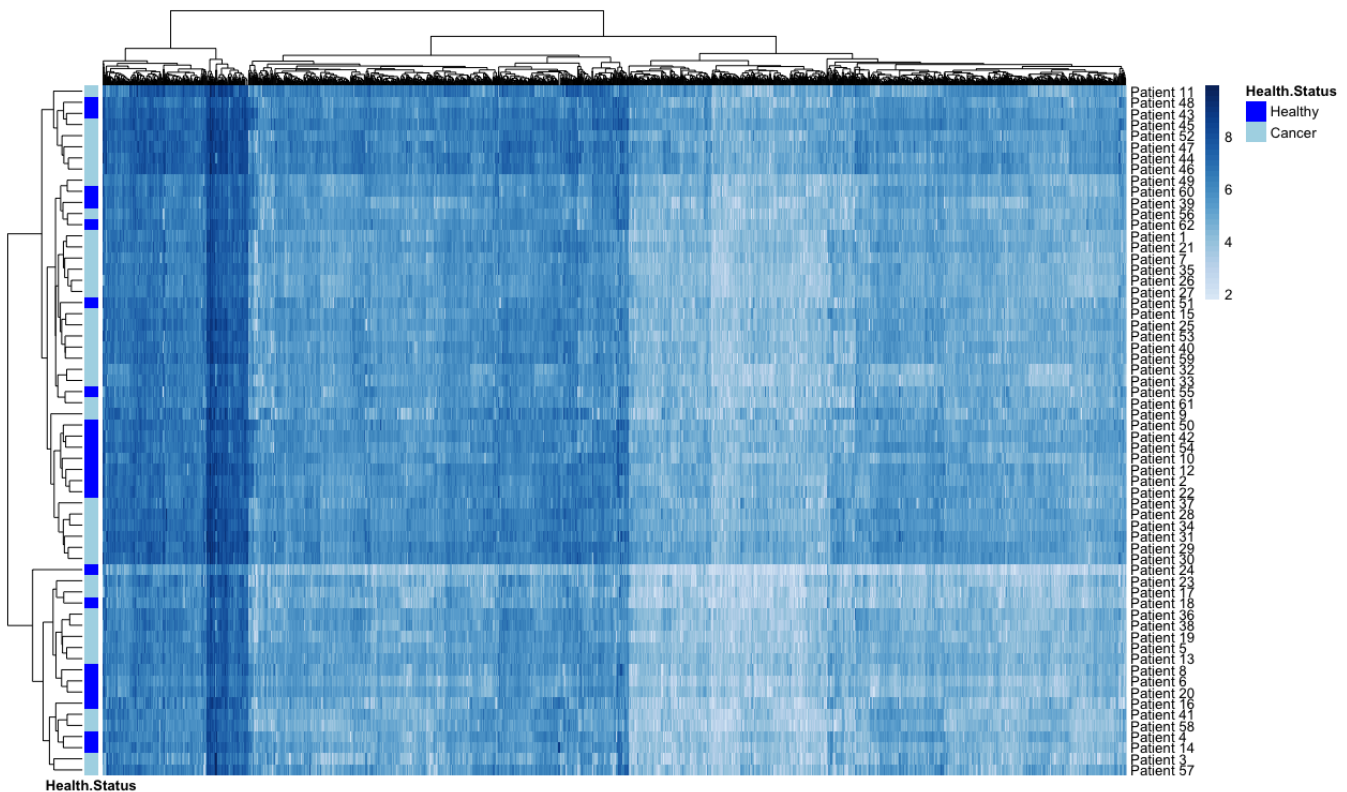


Figure 14: Heatmap of the log values of the Alon microarray dataset. The patients on the rows are stratified according to their health status ("Cancer" vs "Healthy").

We ultimately seek to uncover hidden patterns in this dataset. The task is challenging, especially given the small number of observations available. As a first step, we investigate how well a global estimate of the id can represent the data.

4.1 Homogeneous intrinsic dimension

Let us start with describing the overall complexity of the dataset by computing estimating a homogeneous id value. Using the TWO-NN model, we can compute:

```
R> Alon_twonnn_1 <- twonn(Xalon,method = "linfit")
R> Alon_twonnn_1
```

```
Model: TWO-NN
Method: Least Square Estimation
Sample size: 62, Obs. used: 61. Trimming proportion: 1%
ID estimates (confidence level: 0.95)
```

Lower Bound	Estimate	Upper Bound
-----:	-----:	-----:
10.00382	10.34944	10.69506

```
R> Alon_twonnn_2 <- twonn(Xalon,method = "bayes")
R> Alon_twonnn_2
```

```
Model: TWO-NN
Method: Bayesian Estimation
Sample size: 62, Obs. used: 61. Trimming proportion: 1%
Prior d ~ Gamma(0.001, 0.001)
Credible Interval quantiles: 2.5%, 97.5%
Posterior ID estimates:
```

Lower Bound	Mean	Median	Mode	Upper Bound
-----:	-----:	-----:	-----:	-----:
7.784152	10.17639	10.12084	10.00957	12.88427

```
R> Alon_twonnn_3 <- twonn(Xalon,method = "mle")
R> Alon_twonnn_3
```

```
Model: TWO-NN
Method: MLE
Sample size: 62, Obs. used: 61. Trimming proportion: 1%
ID estimates (confidence level: 0.95)
```

Lower Bound	Estimate	Upper Bound
-----:	-----:	-----:
7.785304	10.01107	12.88623

The estimates based on the TWO-NN model obtained with different methods are very similar. The results are also illustrated in Figure 15, which shows the linear fit (left panel) and posterior distribution (right panel) for the TWO-NN model. According to these results, we conclude that the information contained in the $D = 2000$ genes can be summarized with approximately ten variables. For example, the first ten eigenvalues computed from the spectral decomposition of the matrix $\Lambda = X'_{alon} X_{alon}$ contribute to explain the 95.4% of the total variance.

Although the linear fit plot and the TWO-NN estimates do not raise any evident sign of concern, as a final check, we explore the evolution of the average distances between NN, reported in Figure 16. As expected, the plot does not highlight any abrupt change in the evolution of the ergodic means. However, it suggests that investigating the presence of multiple manifolds could be worthy. In fact, despite the evolution of most of the ergodic means being stationary, the heterogeneous starting points highlight some potential data inhomogeneities that should be

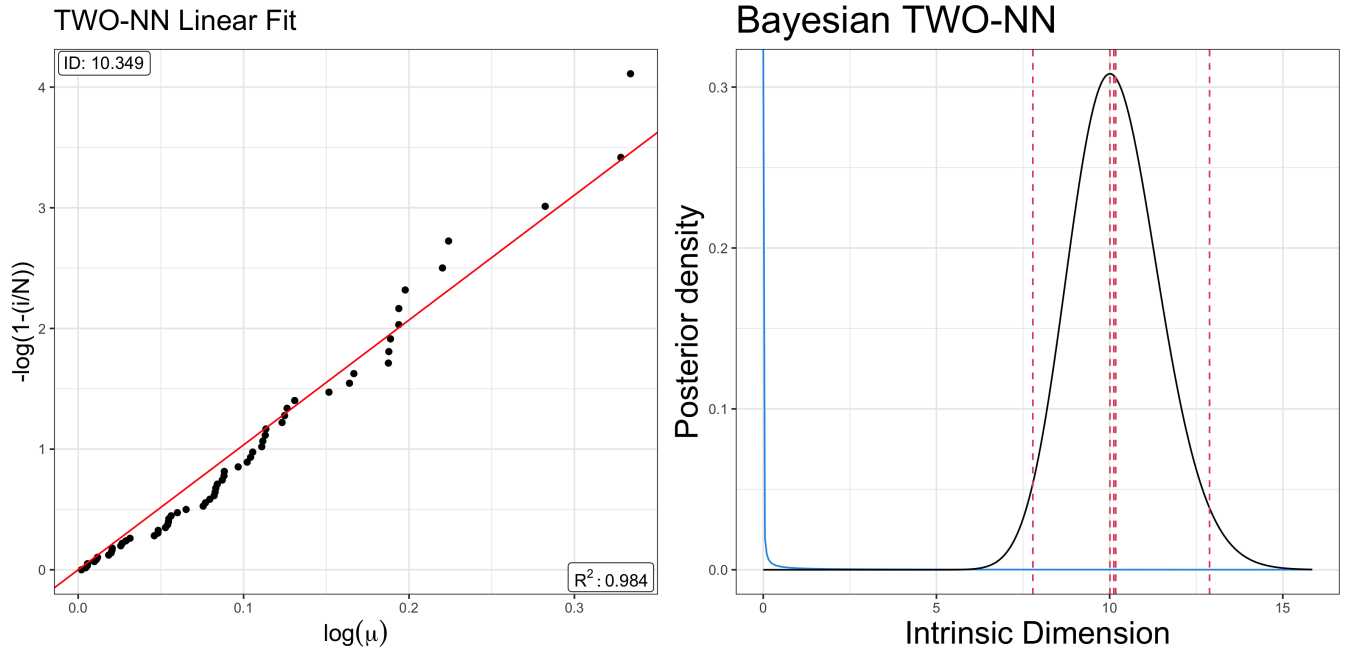


Figure 15: **Alon** dataset. The left panel shows the result of the linear estimator, while the right panel depicts the posterior distribution obtained via the Bayesian approach.

deepen.

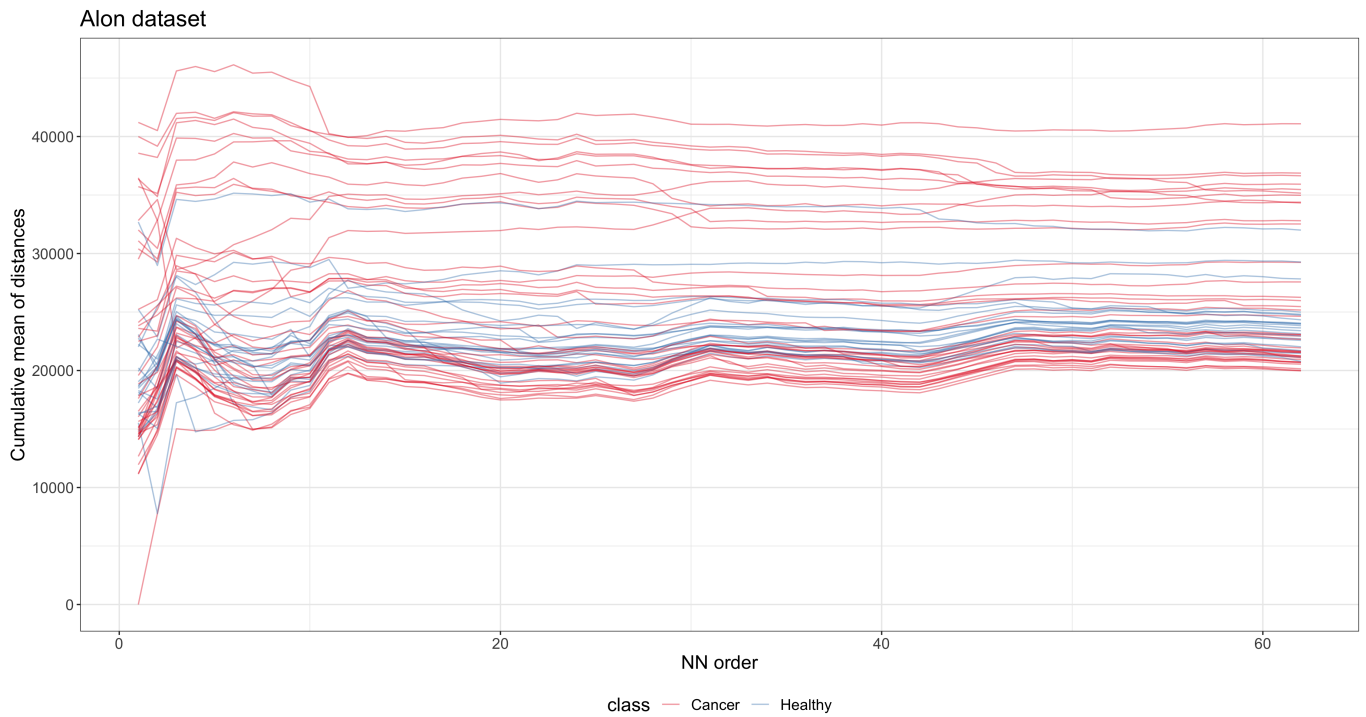


Figure 16: Evolution of the cumulative means of NN distances computed for all the observations in the **Alon** dataset.

4.2 Heterogeneous intrinsic dimension

To investigate the presence of heterogeneous latent manifolds in the `Alon` dataset, we employ `Hidalgo()`. Since the nominal dimension D is large, we do not need to truncate the prior on d . Moreover, given the small number of data points, we opt for an informative and regularizing prior $\text{Gamma}(1, 1)$ instead of the vague default specification. Also, we set a conservative upper bound for the mixing component $K = 30$, and choosing again $\alpha = 0.05$ to fit a sparse mixture. We run:

```
R> set.seed(12345)
R> Alon_hid <- Hidalgo(X = Xalon, K = 30, a0_d = 1, b0_d = 1,
+                       alpha_Dirichlet = .05, nsim = 10000, burn_in = 100000, thin = 5)
R> Alon_hid
```

```
Model: Hidalgo
Method: Bayesian Estimation
Prior d ~ Gamma(1, 1), type = Conjugate
Prior on mixture weights: Dirichlet(0.05) with 30 mixture components
MCMC details:
Total iterations: 110000, Burn in: 1e+05, Elapsed time: 41.1114 secs
```

Once the model is fitted, we first explore the estimated clustering structure. Here, instead of directly plotting the heatmap of the PSM , we build the dendrogram from the dissimilarity matrix obtained as $1 - PSM$, and we report it in the top panel of Figure 17. We construct such plot with the help of the package `ggdendro` [de Vries and Ripley, 2020]. We can detect four clusters, and therefore we decide to set $K = 4$ when running

```
R> Alon_psm <- psm_and_cluster(Alon_hid, K = 4)
```

As illustrated in the previous section, all these plots can be obtained with the proper `autoplot()` specifications. The next natural step is to investigate how strongly the estimated partition, and in general, the estimated `ids`, are associated with health `status`. The bottom two panels of Figure 17 display the boxplots of the values (means and medians) of the `id` stratified by `status` (left) and estimated cluster (right). We can also run

```
R> id_by_class(Alon_hid, class = status)
R> id_by_class(Alon_hid, class = Alon_psm$clust)
```

to obtain summary results linking the variations in the `id` with health status and cluster. We report the results in Table 6. As the estimated `id` increases, the proportion of healthy subjects in each cluster decreases. This result suggests that the microarray profiles of people diagnosed with cancer are slightly more complex than healthy patients' ones.

The analyses conducted so far helped us uncover interesting descriptive characteristics of the `ids` in the dataset. Nevertheless, the results obtained can be effectively used to summarize the data. The estimated individual `id` values are useful to potentially classify the health `status` of new patients according to their genomic profiles. As a simple example, we carry out a classification analysis using two `random forest` models, predicting the target variable $Y = \text{status}$. To train the models, we use two different sets of covariates: `X_0`, the original dataset composed of 2,000 genes,

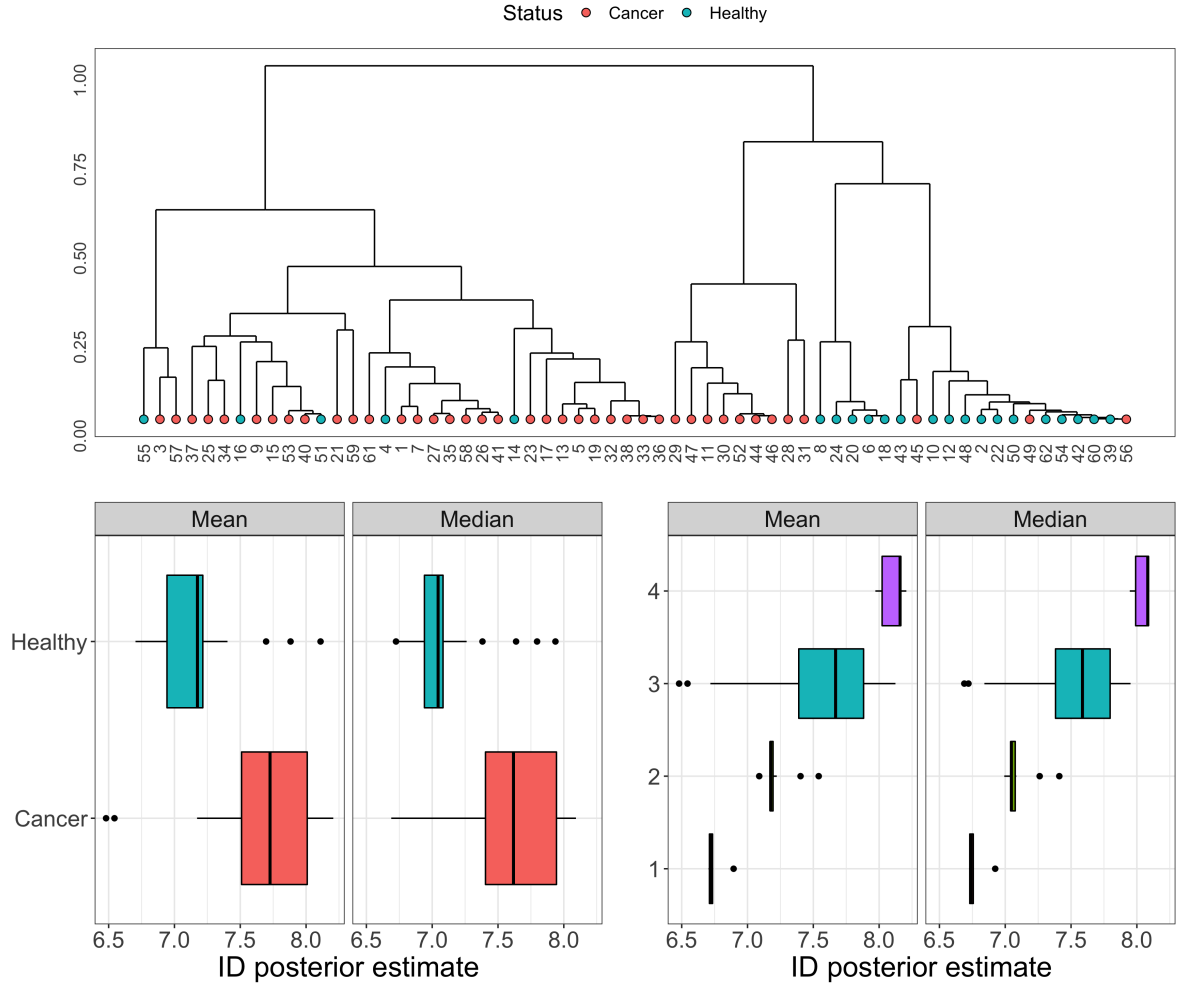


Figure 17: Alon dataset. Top panel: dendrogram obtained from $1 - PSM$. Bottom panel: boxplots of the *id* estimates stratified by health **status** (left) and estimated partition (right).

Cluster	# Cancer	# Healthy	% Healthy	Average id	Median id	Std. Dev.
1	0	5	1.0000	6.7528	6.7206	0.0800
2	3	12	0.8000	7.2140	7.1760	0.1113
3	28	5	0.1515	7.5931	7.6693	0.4145
4	9	0	0.0000	8.1083	8.1593	0.0855

Table 6: Stratification by cluster of the health **status** (in absolute values and proportions of healthy patients) and *id* estimates (median, mean, and standard deviation).

```
R> # Model 1
R> X_0 <- data.frame(Y = status, X = (Xalon))
R> set.seed(123)
R> rfml <- randomForest::randomForest(Y ~ ., data = X_0,
+                                     type = "classification", ntree=100)
```

and *X_I*, the observation-specific *id* summary returned by *Hidalgo()*, along with our estimated

partition.

```
R> # Model 2
R> X_I <- data.frame(Y      = status,
+                   X      = data.frame(Alon_hid$id_summary[, 1:6]),
+                   clust = factor(Alon_psm$clust))
R> set.seed(12315)
R> rfm2 <- randomForest::randomForest(Y ~ ., data = X_I,
+                                     type = "classification", ntree=100)
```

We now inspect the results:

```
R> print(rfm1)
```

Call:

```
randomForest(formula = Y ~ ., data = X_0, type = "classification", ntree = 100)
      Type of random forest: classification
      Number of trees: 100
```

No. of variables tried at each split: 44

OOB estimate of error rate: 24.19%

Confusion matrix:

	Cancer	Healthy	class.error
Cancer	34	6	0.1500000
Healthy	9	13	0.4090909

```
R> print(rfm2)
```

Call:

```
randomForest(formula = Y ~ ., data = X_I, type = "classification", ntree = 100)
      Type of random forest: classification
      Number of trees: 100
```

No. of variables tried at each split: 2

OOB estimate of error rate: 16.13%

Confusion matrix:

	Cancer	Healthy	class.error
Cancer	36	4	0.1000000
Healthy	6	16	0.2727273

Remarkably, a simple dataset with seven variables summarizing the main distributional traits of the observation-specific posterior `ids` obtains better performance in predicting the health `status` than the original dataset. The random forest on the original dataset obtained an out-of-bag estimated error rate of 24.19%, while the error is reduced to 16.13% for our `id`-based dataset. We can conclude that, in this case, the topological properties of the dataset are associated with the outcome of interest and convey important information.

We showed how the estimation of heterogeneous `ids` can not only provide a reliable index of complexity for involved data structures, but can also help unveil relationships among data points hidden at the topological level. The application to the `Alon` dataset showcases how reliable `id` estimates represent a fundamental perspective that help us discover non-trivial data patterns.

Furthermore, one can subsequently exploit the extracted information in many downstream analyses such as patient segmentation or predictive analyses.

5 Summary and discussion

In this paper we introduced and discussed `intRinsic`, an R package that implements novel routines for the `id` estimation according to the models recently developed in [Facco et al. \[2017\]](#), [Allegra et al. \[2020\]](#), [Denti et al. \[2021\]](#), and [Santos-Fernandez et al. \[2021\]](#). `intRinsic` consists of a collection of high-level, user-friendly functions that in turn rely on efficient, low-level routines implemented in R and C++. We also remark that `intRinsic` integrates functionalities from external packages. For example, all the graphical outputs returned by the functions are built using the well-known package `ggplot2`. Therefore, they are easily customizable using the grammar of graphics [\[Wilkinson, 2005\]](#).

To summarize, the package includes both frequentist and Bayesian model specifications for the TWO-NN global `id` estimator. Moreover, it implements the Gibbs sampler for posterior simulation for the `Hidalgo` model, which can capture the presence of heterogeneous manifolds within a single dataset. We showed how the discovery multiple latent manifolds can help unveil topological traits of a dataset by associating the `id` estimates with external variables. As a general analysis pipeline for practitioners, we suggested starting with the efficient TWO-NN functions to understand how appropriate the hypothesis of homogeneity is for the data at hand. If departures from the assumptions are visible from nonuniform estimates obtained with different estimation methods and from visual assessment of the evolution of the average NN distances, one should rely on `Hidalgo`. This model also allows the exploration of relationships between local `id` estimates and external variables.

The most promising future research directions stem from `Hidalgo`. First, we plan to develop more reliable methods to obtain an optimal partition of the data based on the `id` estimates, since the one proposed heavily relies on a mixture model of overlapping distribution. Moreover, another research avenue worth exploring is a version of `Hidalgo` with likelihood distributions based on generalized NN ratios, exploiting the information coming from varying neighborhood sizes.

We are also aware that the mixture model fitting may become time consuming if the analyzed datasets are large. Faster estimating solution via, for example, Variational Bayes approach, will be explored. Also, we highlight that `Hidalgo`, originally proposed as a mixture model within a Bayesian framework, lacks a frequentist-based estimation counterpart such as an Expectation-Maximization algorithm. Its derivation is not immediate, since the neighboring structure introduced via the $\mathcal{N}^{(q)}$ matrix makes the problem non-trivial. We plan to keep working on this package and to continuously update it in the long run, as contributions to this line of research will become available. The novel `id` estimators we discussed have started a lively research branch, and we intend to include all the future advancements in `intRinsic`.

Appendix

A - Additional methods implemented in the package

For the sake of succinctness, we have focused our attention to the discussion of the TWO-NN and the `Hidalgo` models. In Section 2, we explained that both methods are based on the distributional properties of the ratios of distances between the first two NNs of each data point. However, this modeling framework has been extended by [Denti et al. \[2021\]](#), where the authors developed a novel `id` estimator, called `Gride`. This new estimator is based upon the ratios of distances

between NNs of generic order, namely n_1 and n_2 . Extending the neighborhood size leads to two major implications: more stringent local homogeneity assumptions and the possibility to compute estimates as a function of the chosen NN orders. Monitoring the `id` evolution as the order of the furthest NN n_2 increases allows the extraction of meaningful information regarding the link between the `id` and the scale of the considered neighborhood. Doing so, **Gride** produces estimates that are more robust to noise in the dataset, which is not directly addressed by the model formulation.

The **Gride** model is implemented in `intRinsic`, and the estimation can be carried out under both the frequentist and Bayesian frameworks via the function `gride()`, which is very similar to `twonn()` in its usage. Additionally, one can use the functions `twonn_decimation()` and `gride_evolution()` to study the `id` dynamics. More details about these functions are available in the package documentation.

The map in Figure 18 provides a visual summary of the main functions contained in the package. The main topics are reported in the diamonds, while the high-level, exported functions are displayed in the blue rectangles. These routines are linked to the (principal) low-level function via dotted lines. Finally, the light-blue area highlights the functions presented in this paper.

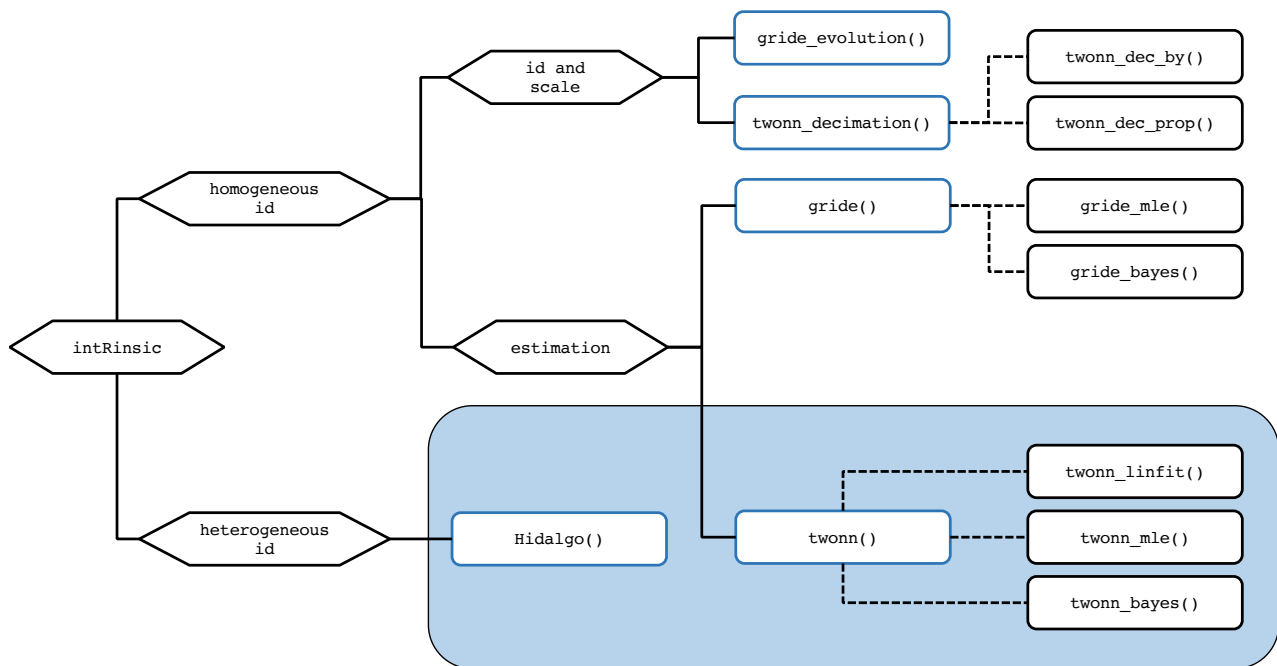


Figure 18: A conceptual map summarizing the most important functions contained in `intRinsic`. The blue squares contain the names of the principal, high-level functions. Dotted lines connect these functions with the most important low-level functions (not exported). The light-blue area represents the topics that have been discussed in this paper.

B - `intRinsic` and other packages

As mentioned in Section 1, there is a large number of intrinsic dimension estimators available in the literature, and many of them have been implemented in R. A valuable survey of the availability of dimensionality reduction methods and `id` estimators have been recently reported in

You [2020a]. From there, we see that two packages are the most important when it comes to `id`: `Rdimtools` and `intrinsicDimension`. `Rdimtools`, in particular, is comprised of an unprecedented collection of methods – including also the least-squares TWO-NN. Such an abundance of methods and the ongoing research in this area indicate that there is no globally optimal estimator to employ regardless of the application. Thus, a practitioner should be aware of the strengths and limitations of every method. Here, we discuss the pros and cons of the methods implemented in `intRinsic`.

At the moment of writing, there are two main traits of `intRinsic` that are unique to this package. First, our package is devoted to the recently proposed likelihood-based estimation methods introduced by the seminal work of Facco et al. [2017] and the literature that followed. Therefore, as of today, most of the implementations presented here are exclusively contained in this package – for example, the R implementation of the `Hidalgo` model and all the routines linked to the `GrIde` family of models. To the best of our knowledge, the function `Hidalgo()` is available outside this package, but it can be only found on GitHub repositories, coded in Python and C++.

Second, all the functions in our package allow – and emphasize – the uncertainty quantification around the `id` estimates, which is an crucial component granted from our model-based approach. This feature is often overlooked in other implementations.

One limitation of the likelihood-based models offered in this package, shared with many other `id` estimators in general, is the underestimation of the `id` when the true latent manifold’s dimension is large. As an empirical rule, for cases where the `id` estimate is large (e.g., $d > 20$), these estimates should be cautiously regarded as lower bounds for the actual value [Ansuini et al., 2019]. An alternative method that we found to be particularly robust to this issue is the Expected Simplex Skewness (ESS) algorithm proposed by Johnsson et al. [2015]. To exemplify, consider 5,000 observations sampled from a $D = d = 50$ dimensional Gaussian distribution. With the following code, we can see how `twonn()` underestimates the true `id`, which is instead well recovered by the ESS.

```
R> set.seed(12211221)
R> X_highdim <- replicate(50, rnorm(5000))
R> intrinsicDimension::essLocalDimEst(X_highdim)

Dimension estimate: 49.05083
Additional data: ess

R> twonn(X_highdim)

Model: TWO-NN
Method: MLE
Sample size: 5000, Obs. used: 4950. Trimming proportion: 1%
ID estimates (confidence level: 0.95)

| Lower Bound| Estimate| Upper Bound|
|-----:|-----:|-----:|
|    34.92154| 35.90791|    36.92254|
```

However, the ESS is not uniformly optimal. For example, for the `Swissroll` data, the `twonn()` performs better:

```
R> intrinsicDimension::essLocalDimEst(Swissroll)
```

```
Dimension estimate: 2.898866
Additional data: ess
```

```
R> twonn(Swissroll, c_trimmed = .001)
```

```
Model: TWO-NN
Method: MLE
Sample size: 1000, Obs. used: 999. Trimming proportion: 0.1%
ID estimates (confidence level: 0.95)
```

Lower Bound	Estimate	Upper Bound
1.945607	2.07005	2.202571

When dealing with dataset characterized by a large number of columns, we suggest checking the discrepancy between our methods and different competitors. A marked difference in the results should flag the likelihood-based findings as less reliable. At this point, a legitimate doubt that may arise regards the validity of the results we derived studying the `Alon` dataset. Because of its high number of columns ($D = 2000$), the intrinsic dimensions we obtained may have been strongly underestimated. To validate our results, we run the ESS estimator on the `Alon` dataset, obtaining

```
R> intrinsicDimension::essLocalDimEst(data = Xalon)
```

```
Dimension estimate: 7.752803
Additional data: ess
```

which is very close to the estimates obtained with our methods, reassuring us about our results.

C - Gibbs Sampler for `Hidalgo()`

The steps of the Gibbs sampler are the following:

1. Sample the mixture weights according to

$$\boldsymbol{\pi} | \dots \sim \text{Dirichlet} \left(\alpha_1 + \sum_{i=1}^n \mathbb{1}_{z_i=1}, \dots, \alpha_K + \sum_{i=1}^n \mathbb{1}_{z_i=K} \right)$$

2. Let \mathbf{z}_{-i} denote the vector \mathbf{z} without its i -th element. Sample the cluster indicators z_i according to:

$$\mathbb{P}(z_i = k | \mathbf{z}_{-i}, \dots) \propto \pi_{z_i} f \left(\mu_i, \mathcal{N}_i^{(q)} | z_1, \dots, z_{i-1}, k, z_{i+1}, \dots, z_n, \mathbf{d} \right)$$

We emphasize that, given the new likelihood we are considering, the cluster labels are no longer independent given all the other parameters. Let us define

$$\mathbf{z}_i^k = (z_1, \dots, z_{i-1}, k, z_{i+1}, \dots, z_n).$$

Then, let $N_{z_i}(\mathbf{z}_{-i})$ be the number of elements in the $(n-1)$ -dimensional vector \mathbf{z}_{-i} that are assigned to the same manifold (mixture component) as z_i . Moreover, let $m_i^{in} =$

$\sum_l \mathcal{N}_{li}^{(q)} \mathbb{1}_{z_l=z_i}$ be the number of points sampled from the same manifold of the i -th observation that have x_i as neighbor, and let $n_i^{in}(\mathbf{z}) = \sum_l \mathcal{N}_{li}^{(q)} \mathbb{1}_{z_l=z_i} \leq q$ be the number of neighbors of x_i sampled from the same manifold. Then, we can simplify the previous formula, obtaining the following full conditional:

$$\begin{aligned} \mathbb{P}(z_i = k | \mathbf{z}_{-i}, \dots) &\propto \frac{\pi_k d_k \mu_i^{-(d_k+1)}}{\mathcal{Z}(\zeta, N_{z_i=k}(\mathbf{z}_{-i}) + 1)} \times \left(\frac{\zeta}{1 - \zeta} \right)^{n_i^{in}(\mathbf{z}_i^k) + m_i^{in}(\mathbf{z}_i^k)} \\ &\times \left(\frac{\mathcal{Z}(\zeta, N_{z_i=k}(\mathbf{z}_{-i}))}{\mathcal{Z}(\zeta, N_{z_i=k}(\mathbf{z}_{-i}) + 1)} \right)^{N_{z_i=k}(\mathbf{z}_{-i})}. \end{aligned} \quad (10)$$

See [Facco and Laio \[2017\]](#) for a detailed derivation of this result.

3. The posterior distribution for \mathbf{d} depends on the prior specification we adopt:

a) If we assume a conjugate Gamma prior, we obtain

$$d_k | \dots \sim \text{Gamma} \left(a_0 + n_k, b_0 + \sum_{i:z_i=k} \log \mu_i \right),$$

where $n_k = \sum_{i=1}^n \mathbb{1}_{z_i=k}$ is the number of observations assigned to the k -th group;

b) If G_0 is assumed to be a truncated Gamma distribution on $(0, D)$, then

$$d_k | \dots \sim \text{Gamma} \left(a_0 + n_k, b_0 + \sum_{i:z_i=k} \log \mu_i \right) \mathbb{1}(\cdot)_{(0,D)};$$

c) Finally, let us define $a^* = a_0 + n_k$ and $b^* = b_0 + \sum_{i:z_i=k} \log \mu_i$, if G_0 is assumed to be a truncated Gamma with point mass at D we obtain

$$d_k | \dots \sim \frac{\hat{\rho}_1^*}{\hat{\rho}_1^* + \hat{\rho}_0^*} \text{Gamma}(a^*, b^*) \mathbb{1}(\cdot)_{(0,D)} + \frac{\hat{\rho}_0^*}{\hat{\rho}_1^* + \hat{\rho}_0^*} \delta_D(d_k),$$

where $\hat{\rho}_1^* = \hat{\rho}^{\mathcal{C}_{a^*,b^*,D}}$ and $\hat{\rho}_0^* = (1 - \hat{\rho}) D^{n_k} \exp^{-D \sum_{i:z_i=k} \log \mu_i}$.

D - Postprocessing to address label switching

The post-processing procedure adopted for the raw chains fitted by `Hidalgo()` works as follows. Let us consider a MCMC sample of length T , and denote a particular MCMC iteration with t , $t = 1, \dots, T$. Let $z_i(t)$ indicate the cluster membership of observation i at the t -th iteration. Similarly, $d_k(t)$ represents the value of the estimated `id` in the k -th mixture component at the t -th iteration. This algorithm maps the K chains for the parameters in \mathbf{d} to each data point via the values of \mathbf{z} . That is, it constructs \mathbf{n} chains, one for each observation, by computing $d_k^*(t) = d_{z_i(t)}(t)$. We then obtain a collection of chains that link every observation to its `id` estimate. When the chains have been post-processed, the local observation-specific `id` can be estimated by the ergodic mean or median.

E - System configuration

We obtained the results in this vignette by running our R code on a MacBook Pro with a 2.6 GHz 6-Core Intel Core i7 processor.

Acknowledgements

The author is extremely grateful to Andrea Gilardi¹ for his valuable comments. The author also thanks Michelle N. Ngo², Derenik Haghverdian², Wendy Rummerfield³, Andrea Cappozzo⁴, and Riccardo Corradin⁵ for their help with the earlier version of this manuscript.

References

- Michele Allegra, Elena Facco, Francesco Denti, Alessandro Laio, and Antonietta Mira. Data segmentation based on the local intrinsic dimension. *Scientific Reports*, 10(1):1–27, 2020. ISSN 20452322. doi: 10.1038/s41598-020-72222-0. URL <https://arxiv.org/abs/1902.10459>.
- U. Alon, N. Barkai, D. A. Notterman, K. Gish, S. Ybarra, D. Mack, and A. J. Levine. Broad patterns of gene expression revealed by clustering analysis of tumor and normal colon tissues probed by oligonucleotide arrays. *Proceedings of the National Academy of Sciences*, 96(12):6745–6750, 1999. ISSN 0027-8424. doi: 10.1073/pnas.96.12.6745.
- Alessio Ansuini, Alessandro Laio, Jakob H. Macke, and Davide Zoccolan. Intrinsic dimension of data representations in deep neural networks. *Advances in Neural Information Processing Systems*, 32, 2019. ISSN 10495258. URL <https://arxiv.org/abs/1905.12784>.
- Christoph Bartenhagen. *RDRToolbox: A package for nonlinear dimension reduction with Isomap and LLE.*, 2020. R package version 1.38.0.
- Robert S. Bennett. The Intrinsic Dimensionality of Signal Collections. *IEEE Transactions on Information Theory*, 15(5):517–525, 1969. ISSN 15579654. doi: 10.1109/TIT.1969.1054365.
- Alina Beygelzimer, Sham Kakadet, John Langford, Sunil Arya, David Mount, and Shengqiao Li. *FNN: Fast Nearest Neighbor Search Algorithms and Applications*, 2019. URL <https://CRAN.R-project.org/package=FNN>. R package version 1.1.3.
- P. Campadelli, E. Casiraghi, C. Ceruti, and A. Rozza. Intrinsic Dimension Estimation: Relevant Techniques and a Benchmark Framework. *Mathematical Problems in Engineering*, 2015, 2015. ISSN 15635147. doi: 10.1155/2015/759567.
- Robrecht Cannoodt and Wouter Saelens. *dyndimred: Dimensionality Reduction Methods in a Common Format*, 2020. URL <https://CRAN.R-project.org/package=dyndimred>. R package version 1.0.3.
- Jose A. Costa and Alfred O. Hero. Geodesic entropic graphs for dimension and entropy estimation in Manifold learning. *IEEE Transactions on Signal Processing*, 52(8):2210–2221, 2004. ISSN 1053587X. doi: 10.1109/TSP.2004.831130.
- David B. Dahl, Devin J. Johnson, and Peter Müller. *salso: Search Algorithms and Loss Functions for Bayesian Clustering*, 2021. URL <https://CRAN.R-project.org/package=salso>. R package version 0.3.0.

¹University of Milan, Bicocca

²University of California, Irvine

³CSU - Eastbay

⁴Politecnico di Milano

⁵University of Nottingham

- Andrie de Vries and Brian D. Ripley. *ggdendro: Create Dendrograms and Tree Diagrams Using 'ggplot2'*, 2020. URL <https://CRAN.R-project.org/package=ggdendro>. R package version 0.1.22.
- Francesco Denti, Diego Doimo, Alessandro Laio, and Antonietta Mira. Distributional Results for Model-Based Intrinsic Dimension Estimators. 2021. URL <https://arxiv.org/abs/2104.13832>.
- Antonio Fabio Di Narzo. *tseriesChaos: Analysis of Nonlinear Time Series*, 2019. URL <https://CRAN.R-project.org/package=tseriesChaos>. R package version 0.1-13.1.
- Dirk Eddelbuettel and Romain François. Rcpp: Seamless R and C++ integration. *Journal of Statistical Software*, 40(8):1–18, 2011. ISSN 15487660. doi: 10.18637/jss.v040.i08.
- Dirk Eddelbuettel and Conrad Sanderson. Rcpparmadillo: Accelerating r with high-performance c++ linear algebra. *Computational Statistics and Data Analysis*, 71:1054–1063, March 2014. URL <https://dx.doi.org/10.1016/j.csda.2013.02.005>.
- Elena Facco and Alessandro Laio. *The intrinsic dimension of biological data landscapes*. PhD thesis, 2017. URL <https://core.ac.uk/download/pdf/144263715.pdf>.
- Elena Facco, Maria D’Errico, Alex Rodriguez, and Alessandro Laio. Estimating the intrinsic dimension of datasets by a minimal neighborhood information. *Scientific Reports*, 7(1):1–8, 2017. ISSN 20452322. doi: 10.1038/s41598-017-11873-y.
- K. Falconer. *Fractal Geometry—Mathematical Foundations and Applications*. John Wiley & Sons, 2nd edition, 2003.
- Constantino A. Garcia. *nonlinearTseries: Nonlinear Time Series Analysis*, 2020. URL <https://CRAN.R-project.org/package=nonlinearTseries>. R package version 0.2.10.
- Jean Golay and Mikhail Kanevski. Unsupervised feature selection based on the Morisita estimator of intrinsic dimension. *Knowledge-Based Systems*, 135:125–134, 2017. ISSN 09507051. doi: 10.1016/j.knosys.2017.08.009.
- Hideitsu Hino. ideo: Intrinsic dimension estimation with R. *R Journal*, 9(2):329–341, 2017. ISSN 20734859. doi: 10.32614/rj-2017-054.
- Hideitsu Hino, Jun Fujiki, Shotaro Akaho, and Noboru Murata. Local intrinsic dimension estimation by generalized linear Modeling. *Neural Computation*, 29(7):1838–1878, 2017. ISSN 1530888X. doi: 10.1162/NECO_a_00969.
- H. Hotelling. Analysis of a complex of statistical variables into principal components. *Journal of Educational Psychology*, 24(7):498–520, 1933. ISSN 00220663. doi: 10.1037/h0070888.
- Kerstin Johnsson and Lund University. *intrinsicDimension: Intrinsic Dimension Estimation*, 2019. URL <https://CRAN.R-project.org/package=intrinsicDimension>. R package version 1.2.0.
- Kerstin Johnsson, Charlotte Soneson, and Magnus Fontes. Low bias local intrinsic dimension estimation from expected simplex skewness. *IEEE Transactions on Pattern Analysis and Machine Intelligence*, 37(1):196–202, 2015. ISSN 01628828. doi: 10.1109/TPAMI.2014.2343220.

- Ian T. Jolliffe and Jorge Cadima. Principal component analysis: A review and recent developments. *Philosophical Transactions of the Royal Society A: Mathematical, Physical and Engineering Sciences*, 374(2065), 2016. ISSN 1364503X. doi: 10.1098/rsta.2015.0202.
- Olga Kayo. Locally Linear Embedding Algorithm Extensions and Applications. 2006. URL internal-pdf://isbn9514280415-4255035408/isbn9514280415.pdf.
- J. F. C. Kingman. *Poisson Processes.*, volume 3. 1992. ISBN 0191591246.
- Guido Kraemer, Markus Reichstein, and Miguel D. Mahecha. dimRed and coRanking—unifying dimensionality reduction in r. *The R Journal*, 10(1):342–358, 2018. URL <https://journal.r-project.org/archive/2018/RJ-2018-039/index.html>. coRanking version 0.2.3.
- Jesse H. Krijthe. *Rtsne: T-Distributed Stochastic Neighbor Embedding using Barnes-Hut Implementation*, 2015. URL <https://github.com/jkrijthe/Rtsne>. R package version 0.15.
- van der Maaten Laurens and Hinton Geoffrey. Visualizing Data using t-SNE. *Journal of Machine Learning Research*, 9:2579–2605, 2009. ISSN 15729338.
- Elizaveta Levina and Peter J Bickel. Maximum Likelihood Estimation of Intrinsic Dimension. In L K Saul, Y Weiss, and L Bottou, editors, *Advances in Neural Information Processing Systems 17*, pages 777–784. MIT Press, 2005. URL <https://papers.nips.cc/paper/2577-maximum-likelihood-estimation-of-intrinsic-dimension.pdf>.
- Gertraud Malsiner-Walli, Sylvia Frühwirth-Schnatter, and Bettina Grün. Model-based clustering based on sparse finite Gaussian mixtures. *Statistics and Computing*, 26(1-2):303–324, 2016. ISSN 15731375. doi: 10.1007/s11222-014-9500-2.
- Gertraud Malsiner-Walli, Sylvia Frühwirth-Schnatter, and Bettina Grün. Identifying Mixtures of Mixtures Using Bayesian Estimation. *Journal of Computational and Graphical Statistics*, 26(2):285–295, 2017. ISSN 15372715. doi: 10.1080/10618600.2016.1200472.
- Thomas Lin Pedersen. *patchwork: The Composer of Plots*, 2020. URL <https://CRAN.R-project.org/package=patchwork>. R package version 1.1.1.
- Karl W. Pettis, Thomas A. Bailey, Anil K. Jain, and Richard C. Dubes. An Intrinsic Dimensionality Estimator from Near-Neighbor Information. *IEEE Transactions on Pattern Analysis and Machine Intelligence*, PAMI-1(1):25–37, 1979. ISSN 01628828. doi: 10.1109/TPAMI.1979.4766873.
- T. S. Roweis and K. Saul Lawrence. Nonlinear Dimensionality Reduction by Locally Linear Embedding. *Science*, 290:2323–2326, 2000.
- Alessandro Rozza, Gabriele Lombardi, Marco Rosa, Elena Casiraghi, and Paola Campadelli. IDEA: Intrinsic dimension estimation algorithm. *Lecture Notes in Computer Science (including subseries Lecture Notes in Artificial Intelligence and Lecture Notes in Bioinformatics)*, 6978 LNCS(PART 1):433–442, 2011. ISSN 03029743. doi: 10.1007/978-3-642-24085-0_45.
- Edgar Santos-Fernandez, Francesco Denti, Kerrie Mengersen, and Antonietta Mira. The role of intrinsic dimension in high-resolution player tracking data – Insights in basketball. *Annals of Applied Statistics - Forthcoming*, 2021. ISSN 2331-8422. URL <https://arxiv.org/abs/2002.04148>.

- Hana Sevcikova, Don Percival, and Tilmann Gneiting. *fractaldim: Estimation of fractal dimensions*, 2014. URL <https://CRAN.R-project.org/package=fractaldim>. R package version 0.8-4.
- J. B. Tenenbaum, V. De Silva, and J. C. Langford. A global geometric framework for nonlinear dimensionality reduction. *Science*, 290(5500):2319–2323, 2000. ISSN 00368075. doi: 10.1126/science.290.5500.2319.
- Hadley Wickham. *ggplot2: Elegant Graphics for Data Analysis*. Springer-Verlag New York, 2016. ISBN 978-3-319-24277-4. URL <https://ggplot2.tidyverse.org>.
- Leland Wilkinson. *The Grammar of Graphics*, volume 95. Springer-Verlag, 2005.
- Kisung You. Rdimtools: An R package for Dimension Reduction and Intrinsic Dimension Estimation. *arXiv*, 2020a.
- Kisung You. *Rdimtools: Dimension Reduction and Estimation Methods*, 2020b. URL <https://CRAN.R-project.org/package=Rdimtools>. R package version 1.0.4.